JOHANNES KEPLER
UNIVERSITÄT LINZ
Netzwerk für Forschung, Lehre und Praxis

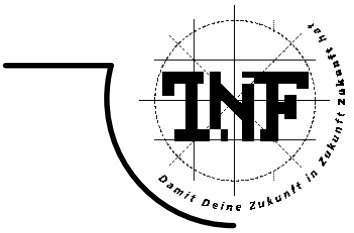

Fourier Analysis and Local Fourier Analysis for Multigrid Methods

Master's Thesis

for obtaining the academic title

Master of Science

in

INTERNATIONALER UNIVERSITÄSLEHRGANG

INFORMATICS: ENGINEERING & MANAGEMENT

composed at ISI-Hagenberg

Handed in by:

Yao Zhou, 0856068

Finished on:

July 9th, 2009

Scientific Advisor:

O. Univ. Prof. Dipl. Ing. Dr. Ulrich. Langer.

Hagenberg, July 2009

Abstract

The aim of this master thesis is to apply Fourier analysis and local Fourier analysis (LFA) to calculate the exact convergence factor of two-grid methods for the solution of linear algebraic systems arising in different applications. We first consider the one-dimensional Poisson problem. Both Fourier analysis and LFA are used to derive two-grid convergence factors. Differences between these two analysis tools are illustrated. Then we study a saddle-point problem stemming from an optimal control problem. The smoothing factor for the optimal control problem is derived by Fourier analysis for a special preconditioner. Moreover, the robustness of the preconditioner is shown by the numerical experiment. In the conclusion we summarize the results and give an outlook to further investigation. In particular, we are interested in the Fourier analysis for a mixed formulation of the biharmonic equation that leads to a system of finite element equations that is quite similar to the system arising from the optimal control problem.

Acknowledgments

First of all I would like to express my deep gratitude to Prof. Bruno Buchberger for giving me this great opportunity to study at the International School for Informatics and many thanks for all he tried and did for us. What I have learned from ISI and Prof. Buchberger is a precious experience that will inspire me for all the rest of my life. I would like to thank all those who were actively involved in coordinating the activities of ISI, especially Betina Curtis, making my one year study in Austria enjoyable and comfortable.

I am very grateful to my supervisor Prof. Ulrich Langer, for guiding and encouraging me during my work on the master thesis. I would also like to thank Prof. Walter Zulehner and Dr. Georg Regensburger for discussions on my work.

In particular, I want to thank my friend Dr. Xiliang Lu for his valuable contributions and strong help.

I want to acknowledge Johann Radon Institute for Computational and Applied Mathematics (RICAM) for offering me this chance to writing my master's thesis and for supporting my studies and stay in Austria.

I profoundly thank and appreciate very much the efforts of my parents, my grandparents and my boyfriend, who always supported me in my choices. I am grateful to my college Le Wang who encouraged me a lot and other friends who also participate in the ISI2008 program for sharing the difficulties and happiness with me.

Yao Zhou
Linz, July 2009

Contents

Chapter 1

Introduction

The main goal of this work is to apply Fourier analysis and local Fourier analysis (LFA) to calculate the convergence rate of multigrid methods for solving linear system of equations coming from the finite element discretization of partial differential equations.

The discretization of partial differential equations leads to very large systems of equations. For instance, in three space dimensions, more than one million unknowns can be reached very easily. The direct solution of systems of this size is prohibitively expensive, both with respect to the amount of storage and to the computational work. Therefore iterative methods like the Gauss-Seidel or the Jacobi iteration have been widely used from the beginning of the numerical treatment of partial differential equations.

An important step was Young's successive over-relaxation method [28] (1950) which is much faster than the closely related Gauss-Seidel iteration. Nevertheless, this method shares with direct elimination methods the disadvantage that the amount of work does not remain proportional to the number of unknowns; the computer time needed to solve a problem grows more rapidly than the size of the problem.

Multigrid methods were the first to overcome this complexity barrier. Multigrid algorithms are composed of four elements:

(1) smoothing of rough error parts via classical iterative methods;

(2) approximation of smooth errors on a coarser grid;

(3) recursive application of (1) and (2) on a sequence of coarser and coarser grids;

(4) nested iteration for producing good initial guesses.

In 1961, Fedorenko proposed the first two-grid method (elements (1) and (2)) in his pioneering paper [11] for solving the finite difference equations arising from the

five-point approximation of the Poisson equation in a rectangular domain. Already the first numerical results presented in this paper showed the great potential of this method. In his second paper [12] from 1964, he gave a first convergence analysis and proposed to combine (1) and (2) with (3) that results in a complete multigrid cycle. In 1966, Bakhvalov provided the first rigorous convergence proof on the basis of the sum splitting technique and showed that the nested iteration technique with the multigrid as nested iteration process allows us to produce approximate solutions that differ from the exact solution of the boundary value problem in the order of the discretization error with optimal complexity [2]. In the 1970s, these techniques were generalized to variational finite difference equations and general finite element equations by Astrakhantsev [1] and by Korneev [20], respectively.

The paper of Brandt [6] and the report of Hackbusch [13] were the historical break through. They reinvented the multigrid method independently of the Russian school, generalized it to new classes of problems, and developed the theory. In his first two papers [4, 5] (1973, 1976) and then summarized in the systematic 1977 work [6], Brandt showed the actual efficiency of multigrid methods. His essential contributions (in the early studies) include the introduction of a nonlinear multigrid method (FAS) and of adaptive techniques (MLAT), the discussion of general domains, the systematic application of the nested iteration idea (FMG) and, last but not least, the introduction of the Local Fourier Analysis as a tool for theoretical investigation and method design. Hackbusch's first systematic report [13] (1976) contains many theoretical and practical investigations such as Fourier analysis considerations which have been taken up and developed further by several authors. In the papers [14, 15, 16], Hackbusch then presented a general convergence theory of multigrid methods. The first big multigrid conference in 1981 in Cologne was a culmination point of the development; the conference proceedings edited by Hackbusch and Trottenberg [17] are still a basic reference. The first monograph on multigrid methods was published by Hackbusch in 1985 [18]. In this monograph, the reader finds a complete overview of the most important results on multigrid and related methods obtained till 1985.

Today, multigrid methods are used in nearly every field where partial differential equations are solved by numerical methods. After the pioneering monograph [18] by Hackbusch, many further books have been published wherein one can find interesting additional information on the theory and application of multigrid methods in survey form, e.g. the books by Briggs, Henson and McCormick [10], Bramble [3], Wesseling [26], Trottenberg, Oosterlee and Schüller [25]. The most recent information about publications on multigrid method, related conferences, multigrid software, etc., can be found on the multigrid home page http://www.mgnet.org on the internet.

Considering multigrid algorithms, there is an enormous degree of freedom in choosing the algorithmic components. The practical very important question is how to choose individual multigrid components for concrete situations. There are two related approaches in treating this question: Fourier analysis and local Fourier analysis (LFA). They are considered as the main analysis tools to obtain quantitative convergence es-

timates and to optimize multigrid components like smoothers or intergrid transfer operators.

In Fourier analysis and LFA, the discrete solution and the corresponding error can be represented by linear combinations of certain functions, which form a unitary basis of the space of grid functions with bounded l_2-norm. However, in Fourier analysis we use the exact eigenfunctions of the discrete operator which are compatible with the boundary conditions. Whereas in LFA an infinite grid is considered and boundary conditions are not taken into account. In this case, we use exponential functions instead of the exact eigenfunctions. Both ideas were introduced by Brandt [6] and afterward extended and refined in [7, 9]. A good introduction can be found in the paper by Stüben and Trottenberg [21] and in the books by Wesseling [26], Trottenberg et al. [25] and Wienands and Joppich [27]. In particular, the book by Wienands and Joppich [27] provides with the software package **LFA** for local Fourier Analysis.

The paper is organized as follows: In Chapter 2 we introduce the basic ideas of multigrid methods and illustrate the multigrid algorithm. Chapter 3 serves as a demonstration of how model problem can be investigated by means of Fourier analysis and LFA. Connections and differences of these two analysis tools are described. The main part of the paper is the application to PDE-constrained optimization problem in Chapter 4, both Fourier analysis and LFA are applied to compute the two-grid convergence rate and also numerical results are presented. In Chapter 5 we summarize the results and conclude with some remarks about possible continuation.

Chapter 2

Multigrid Methods

Multigrid methods are among the fastest numerical algorithms for solving linear systems arising from a discretization technique such as the finite element method or the finite difference method. The convergence speed does not deteriorate when the discretization is refined, whereas classical iterative methods slow down for decreasing mesh size. For a wide overview about multigrid methods we recommend the books Hackbusch and Trottenberg [19], Hackbusch [18], Bramble [3] and Trottenberg, Oosterlee and Schüller [25].

The starting point of the multigrid idea is the observation that classical iteration methods (like the Gauss-Seidel iteration and the damped Jacobi method) have smoothing properties. Although these methods are characterized by poor global convergence rates, for errors whose length scales are comparable to the mesh size, they provide rapid damping, leaving behind smooth, longer wave-length errors. These smooth parts of the error are responsible for the poor convergence. A (geometric) multigrid method involves a hierarchy of meshes and related discretizations. A quantity that is smooth on a certain grid can, without any essential loss of information, also be approximated on a coarser grid. So the low-frequency error components can be effectively reduced by a coarse-grid correction procedure. Because the action of a smoothing iteration leaves only smooth error components, it is possible to represent them as the solution of an appropriate coarser system. Once this coarser problem is solved, its solution is interpolated back to the fine grid to correct the fine grid approximation for its low-frequency errors.

Thus, the multigrid idea is based on two principles: error smoothing and coarse grid correction. In this chapter, we will explain how these principles are combined to form a multigrid algorithm. The basics of multigrid methods will be described systematically.

In Section 2.1 , we discuss the smoothing properties of one classical iterative solver, typically the Jacobi method. The concrete example refers to Poisson's equation. Sections 2.2 and 2.3 give a systematic introduction to two-grid iteration and multigrid iteration, respectively.

2.1 Motivation

2.1.1 Model Problem

A natural model of an elliptic equation is the two-dimensional Poisson equation in a square. However, the analysis of classical iterative methods as well as the multigrid algorithm for this problem is not sufficiently transparent for an introductory consideration. Therefore, we start with the simplest *one*-dimensional Dirichlet boundary value problem

$$-u(x)'' = f(x) \quad \text{in} \quad \Omega = (0,1), \quad u(x) = 0 \quad \text{at} \quad x \in \Gamma = \{0,1\}. \tag{2.1}$$

Discretising the model problem by finite element method with piecewise linear, continuous functions we obtain a linear system of equations

$$K_h \underline{u}_h = \underline{f}_h, \tag{2.2}$$

with the tridiagonal matrix

$$K_h = \frac{1}{h} \begin{bmatrix} 2 & -1 & & & \\ -1 & 2 & -1 & & \\ & -1 & \ddots & \ddots & \\ & & \ddots & \ddots & -1 \\ & & & -1 & 2 \end{bmatrix}_{(n-1)\times(n-1)} \tag{2.3}$$

and the vectors

$$\underline{u}_h = (u_h(jh))_{j=1}^{n-1}, \quad \underline{f}_h = (f_h(jh))_{j=1}^{n-1}.$$

The boundary conditions $u_h(0) = u_h(1) = 0$ are incorporated into the system.

Here h denotes the grid size. The grid Ω_h corresponding to $h = 1/n$ consists of the points $x_j = jh\,(j = 1, \ldots, n-1)$. From the beginning we introduce not only one grid but a hierarchy of grids. The largest possible grid size is $h_0 = 1/2$. The corresponding grid Ω_0 consists of the single grid point $x_1 = 1/2$. The next finer grid should be defined by halving the step size (standard coarsening): $h_1 = \frac{1}{4}$. Thus, this refinement process yields the sequence

$$h_0 > h_1 > h_2 \ldots > h_l \ldots \quad \text{with} \quad h_l = 2^{-1-l}. \tag{2.4}$$

The subscript l is called the *level number*. In this paper, we assume that n is an even number and choose Ω_H with mesh size $H = 2h$ to be the coarse grid.

2.1.2 Convergence Analysis for the ω-Jacobi Iteration

The asymptotic convergence property of an iterative method is characterized by the spectral radius of its corresponding operator

$$\rho(S_h) = \max\{|\lambda| \ : \ \lambda \text{ is eigenvalue of } S_h\}$$

which is also called the asymptotic convergence factor. The iterative process converges if and only if $\rho(S_h) < 1$.

For model problem (2.1), the ω-Jacobi method reads

$$\underline{u}_h^{j+1} = \underline{u}_h^j + \frac{\omega h}{2}(\underline{f}_h - K_h \underline{u}_h^j). \tag{2.5}$$

Clearly, the corresponding iteration operator is given by

$$S_h = S_h(\omega) = I - \frac{\omega h}{2} K_h. \tag{2.6}$$

The spectral radius of the iteration operator for the Jacobi method can be determined analytically for our model problem. The first step is to verify that

$$\varphi_h^k = (\sqrt{2h}\sin(k\pi x_j))_{j=1}^{n-1} = (\sqrt{2h}\sin(kj\pi h))_{j=1}^{n-1} \quad k = 1, ..., n-1. \tag{2.7}$$

and

$$\lambda_h^k = \frac{4}{h}\sin^2(\frac{1}{2}k\pi h) \tag{2.8}$$

are eigenfunctions, respectively eigenvalues of K_h.

The eigenfunctions of S_h are the same as those of K_h. The corresponding eigenvalues of S_h are

$$\lambda_h^k(S_h) = 1 - \frac{\omega h}{2}\lambda_h^k = 1 - 2\omega\sin^2(\frac{1}{2}k\pi h) = 1 - \omega + \omega\cos k\pi h. \tag{2.9}$$

For the spectral radius $\rho(S_h) = \rho(h, \omega) = \max\{|\lambda_h^k(\omega)| : k = 1, \ldots, n-1\}$, we obtain

$$\begin{aligned} \text{for} \quad 0 < \omega \leq 1 : \rho(S_h(\omega)) &= |\lambda_h^1(\omega)| = 1 - \omega + \omega\cos\pi h = 1 - O(h^2), \\ \text{else} : \rho(S_h) &\geq 1 \quad (\text{for } h \text{ small enough}). \end{aligned} \tag{2.10}$$

Thus, the choice $\omega \in (0, 1]$ implies convergence. However, the spectral radius is very close to one if h is small and there is no satisfactory convergence for any ω. We can easily spot the *h-dependent convergence*: the smaller h becomes the worse the convergence is.

2.1.3 Smoothing Properties of ω-Jacobi Relaxation

The situation is quite different with respect to the *smoothing properties* of ω-Jacobi relaxation. For $0 < \omega \leq 1$, we first observe by (2.10) that it is the smoothest eigenfunction φ_h^1 which is responsible for the slow convergence of Jacobi's method. Highly oscillating eigenfunctions are reduced much faster if ω *is chosen properly*. The construction of the multigrid iteration is based on this observation.

To see this, we consider the approximations before ($\underline{w}_h$) and after ($\underline{\bar{w}}_h$) one relaxation step. Since the eigenfunctions φ_h^k of the iteration operator form a basis for all

grid functions having zero boundary values, we can expand the errors before and after one relaxation step, namely

$$\underline{v}_h := \underline{u}_h - \underline{w}_h \quad \text{and} \quad \bar{\underline{v}}_h := \underline{u}_h - \bar{\underline{w}}_h$$

into discrete eigenfunction series:

$$\underline{v}_h = \sum_{k=1}^{n-1} \alpha_k \varphi_h^k, \quad \bar{\underline{v}}_h = \sum_{k=1}^{n-1} \lambda_h^k(S_h(\omega))\alpha_k \varphi_h^k \tag{2.11}$$

In order to analyze the smoothing properties of $S_h(\omega)$ we distinguish *low* and *high* frequencies (with respect to the coarser grid Ω_H used). For the definition of the high and low frequencies, we return to the eigenfunctions φ_h^k in (2.7). For given k, we consider the eigenfunctions

$$\varphi_h^k, \qquad \varphi_h^{n-k}$$

and observe that they coincide on Ω_H in the following sense:

$$\varphi_h^k(x_j) = -\varphi_h^{n-k}(x_j) \quad \text{for} \quad x_j \in \Omega_H. \tag{2.12}$$

This means that these two eigenfunctions cannot be distinguished on Ω_H. (For $k = n/2$, the φ_h^k vanishes on Ω_H.) This gives rise to the following definition of low and high frequencies:

Definition 2.1. (in the context of model problem)

$$\begin{aligned} &\text{low frequencies} : \varphi_h^k \quad \text{with} \quad k < n/2, \\ &\text{high frequencies} : \varphi_h^k \quad \text{with} \quad n/2 \le k < n. \end{aligned} \tag{2.13}$$

Obviously, only the low frequencies are representable on the coarser grid Ω_H. The high frequencies are *not visible* on Ω_H since either they coincide with a low frequency on Ω_H or vanish on Ω_H.

In order to measure the smoothing properties of $S_h(\omega)$ quantitatively, we now introduce the *smoothing factor* $\mu(h;\omega)$ of $S_h(\omega)$ (and its supremum $\mu^*(\omega)$ over h) as follows:

Definition 2.2. Smoothing factor (of ω-Jacobi for model problem)
The *smoothing factor* $\mu(h;\omega)$ of $S_h(\omega)$, representing the worst factor by which *high frequency* error components are reduced per relaxation step, and its supremum μ^* *over* h, are defined as

$$\begin{aligned} \mu(h;\omega) &:= \max\{|\lambda_h^k(S_h(\omega))| : n/2 < k \le n-1\}, \\ \mu^*(\omega) &:= \sup\{\mu(h;\omega) : h \le 1/2\} \end{aligned} \tag{2.14}$$

Inserting (2.9), we obtain from (2.14)

$$\begin{aligned} \mu(h;\omega) &= \max\{|1-\omega|, |1-\omega(1+\cos\pi h)|\}, \\ \mu^*(\omega) &= \max\{|1-\omega|, |1-2\omega|\} \end{aligned} \tag{2.15}$$

This shows that Jacobi's relaxation has no smoothing properties for $\omega \leq 0$ or $\omega > 1$:

$$\mu(h;\omega) \geq 1 \text{ if } \omega \leq 0 \text{ or } \omega > 1 \quad (\text{and } h \text{ sufficiently small})$$

For $0 < \omega < 1$, however, the smoothing factor is smaller than 1 and bounded away from 1, independently of h. For $\omega = 1$, we have a smoothing factor of $1 - O(h^2)$ only. In particular, we find from (2.15) that

$$\mu(h;\omega) = \begin{cases} \cos\pi h & \text{if } \omega = 1 \\ 1/2 & \text{if } \omega = 1/2 \\ 1/3 & \text{if } \omega = 2/3 \end{cases} \qquad \mu^*(\omega) = \begin{cases} 1 & \text{if } \omega = 1 \\ 1/2 & \text{if } \omega = 1/2 \\ 1/3 & \text{if } \omega = 2/3 \end{cases}$$

The choice $\omega = 2/3$ is optimal in the following sense:

$$\inf\{\mu^*(\omega) : 0 \leq \omega \leq 1\} = \mu^*(\frac{2}{3}) = \frac{1}{3}. \tag{2.16}$$

With respect to $\mu(h;\omega)$, we obtain

$$\inf\{\mu(h;\omega) : 0 \leq \omega \leq 1\} = \mu(h; \frac{2}{2+\cos\pi h}) = \frac{\cos\pi h}{2+\cos\pi h} = \frac{1}{3} - |O(h^2)|.$$

This means that one step of ω-Jacobi with $\omega = 2/3$ reduces all high frequency error components by at least a factor of 1/3 (independent of the grid size h).

The above consideration is an example of what we call *smoothing analysis*.

2.2 Two-Grid Method

The foregoing section showed that the simple ω-Jacobi iteration (2.5) with a properly chosen ω is quite an efficient method for reducing the high-frequency components. Convergence is only lacking with respect to low frequencies (smooth components). Therefore, one should combine this iteration with a second one having complementary properties. In particular, the second iteration should reduce the smooth error very well. Such a complementary iteration can be constructed by means of the coarse grid with step size $h_{l-1} = 2h_l$. For our model problem, we use $H = 2h$.

Let $\underline{u}_h^{old}$ be some given approximation to $\underline{u}_h = K_h \underline{f}_h$. A small number of iterations of method (2.5) will result in an intermediate value $\bar{\underline{u}}_h$. From the previous section we know that the error $\underline{v}_h = \underline{u}_h - \bar{\underline{u}}_h$ is smooth (more precisely, smoother than $\underline{u}_h - \underline{u}_h^{old}$). $\underline{v}_h$ can also be regarded as the exact correction since $\underline{u}_h = \bar{\underline{u}}_h + \underline{v}_h$.

Inserting $\underline{u}_h$ into the equation $K_h \underline{u}_h = \underline{f}_h$ we obtain the *defect*

$$\underline{d}_h = \underline{f}_h - K_h \bar{\underline{u}}_h \tag{2.17}$$

of $\bar{\underline{u}}_h$, which vanishes if and only if $\bar{\underline{u}}_h$ is the exact solution $\underline{u}_h$. Because of $K_h\underline{v}_h = K_h\bar{\underline{u}}_h - K_h\underline{u}_h = K_h\bar{\underline{u}}_h - \underline{f}_h$ the exact correction $\underline{v}_h$ is the solution of

$$K_h\underline{v}_h = \underline{d}_h. \tag{2.18}$$

The *defect* equation (2.18) is equivalent to the original equation (2.2). The *exact* solution of the *defect* equation is as difficult as for the original one. Nevertheless, $\underline{v}_h$ can be *approximated* better by means of a coarser grid than $\underline{u}_h$, since $\underline{v}_h$ is a smooth grid function and only smooth functions can be represented well by means of coarser grids.

To approximate the problem (2.18) by a coarse grid equation

$$K_H\underline{v}_H = \underline{d}_H \tag{2.19}$$

we have to choose d_H reasonably. Note that the matrix K_H is already defined by the underlying bilinear form and the basis functions of the coarse finite dimensional space V_H. We define $\underline{d}_H$ as the restriction of the fine grid defect to the coarse grid, that is

$$\underline{d}_H = I_h^H\underline{d}_h \tag{2.20}$$

Here I_h^H is called the *restriction*. For our model problem we use the weighted restriction given by

$$I_h^H d_h(x) = \frac{1}{2}d_h(x-h) + d_h(x) + \frac{1}{2}d_h(x+h), \quad \text{for } x \in \Omega_H \tag{2.21}$$

The corresponding matrix is

$$I_h^H = \frac{1}{2}\begin{bmatrix} 1 & 2 & 1 & & & & & O & & \\ & & 1 & 2 & 1 & & & & & \\ & & & & & \ddots & & & & \\ & & & & & & 1 & 2 & 1 & \\ & & O & & & & & 1 & 2 & 1 \end{bmatrix}_{(\frac{n}{2}-1)\times(n-1)} \tag{2.22}$$

Having defined $\underline{d}_H$ by (2.20) from the defect $\underline{d}_h$, we obtain the exact solution $\underline{v}_H$ of the coarse grid equation (2.19). Reasonably one expects $\underline{v}_H$ to be an approximation to the exact correction $\underline{v}_h$. However $\underline{v}_H$ is only defined on the coarse grid Ω_H. We have to interpolate this coarse grid function by

$$\hat{\underline{v}}_h = I_H^h\underline{v}_H, \tag{2.23}$$

where I_H^h is called the *prolongation*. The simplest example for a prolongation operator is the linear interpolation

$$I_H^h v_H(x) = \begin{cases} v_H(x) & \text{if } x \in \Omega_H \\ \frac{1}{2}\left[v_H(x-h) + v_H(x+h)\right] & \text{otherwise.} \end{cases} \tag{2.24}$$

The corresponding matrix is

$$\mathrm{I}_{\mathrm{H}}^{\mathrm{h}} = \frac{1}{2}\begin{bmatrix} 1 & & & & & \\ 2 & & & & & \\ 1 & 1 & & & & \\ & 2 & & & & \\ & & \ddots & & & \\ & & & 2 & & \\ & & & 1 & 1 & \\ & & & & 2 & \\ & & & & 1 & \end{bmatrix}_{(n-1)\times(\frac{n}{2}-1)} \tag{2.25}$$

Since $\underline{u}_h = \bar{\underline{u}} + \underline{v}_h$ is the exact solution and $\hat{\underline{v}}_h = I_H^h \underline{v}_H$ is supposed to approximate $\underline{v}_h$, we update the value $\bar{\underline{u}}_h$ by

$$\underline{u}_h^{new} = \bar{\underline{u}}_h + \hat{\underline{v}}_h. \tag{2.26}$$

All steps from $\hat{\underline{u}}_h$ to $\underline{u}_h^{new}$ by (2.18)-(2.26) can be combined into the so-called *coarse grid correction* step

$$\underline{u}_h^{new} = \bar{\underline{u}}_h - I_H^h K_H^{-1} I_h^H (K_h \bar{\underline{u}}_h - \underline{f}_h). \tag{2.27}$$

The associated iteration operator is given by

$$M_h^{CGC} = I - I_H^h K_H^{-1} I_h^H K_h. \tag{2.28}$$

Remark 2.3. *Taken on its own, the coarse grid correction process (2.27) is of no use. It is not convergent! We have*

$$\rho(M_h^{CGC}) \geq 1. \tag{2.29}$$

This remark follows directly from the fact that the restriction I_h^H has a nontrivial kernel. If we choose $0 \neq \underline{z}_h \in ker(I_h^H)$ and set $\underline{u}_h^0 := K_h^{-1}(\underline{f}_h - \underline{z}_h)$. As $\underline{d}_h = \underline{z}_h$ and $\underline{z}_H = I_h^H \underline{z}_h = 0$, the resulting iterates are $\underline{u}_h^j = \underline{u}_h^0$. The solution will not be changed by a pure coarse grid correction.

It is the combination of smoothing iteration and coarse-grid correction that is rapidly convergent, whereas both components by themselves converge slowly or not at all. The combination is called a *two-grid method* since two levels h and H are involved. Each iteration of a two-grid method consists of a *smoothing* and a *coarse grid correction* part.

One step of such a two-grid method (calculating $\underline{u}_h^{j+1}$ from $\underline{u}_h^j$) proceeds as follows:

Two-grid method $\underline{u}_h^{j+1} = TGM^{(\nu_1,\nu_2)}(\underline{u}_h^j, K_h, \underline{f}_h, \nu_1, \nu_2)$

(1) Presmoothing

- Compute $\bar{\underline{u}}_h^j$ by applying $\nu_1 (\geq 0)$ steps of a given smoothing method to $\underline{u}_h^j$:

$$\bar{\underline{u}}_h^j = S_h^{\nu_1}(\underline{u}_h^j, K_h, \underline{f}_h)$$

(2) Coarse grid correction (CGC)

- Compute the defect: $\underline{d}_h^j = \underline{f}_h - K_h \bar{\underline{u}}_h^j.$
- Restrict the defect (fine-to-coarse transfer): $\underline{d}_H^j = I_h^H \underline{d}_h^j.$
- Solve exactly on Ω_H: $K_H \underline{v}_H = \underline{d}_H^j.$
- Interpolate the correction (coarse-to-fine transfer): $\underline{v}_h = I_H^h \underline{v}_H$
- Compute the corrected approximation: $\hat{\underline{u}}_h = \bar{\underline{u}}_h^j + \underline{v}_h$

(3) Postsmoothing

- Compute $\underline{u}_h^{j+1}$ by applying $\nu_2 (\geq 0)$ steps of the given smoothing method to $\hat{\underline{u}}_h$:

$$\underline{u}_h^{j+1} = S_h^{\nu_2}(\hat{\underline{u}}_h, K_h, \underline{f}_h)$$

From the above description, we immediately obtain the iteration operator M_h^{TGM} of the (h, H) two-grid method:

$$M_h^{TGM} = S_h^{\nu_2} M_h^{CGC} S_h^{\nu_1} = S_h^{\nu_2}(I - I_H^h K_H^{-1} I_h^H K_h) S_h^{\nu_1}. \tag{2.30}$$

2.3 Multigrid Method

Up to now, we have described the multigrid principle only in its two-grid version. However, the two-grid methods usually are not used in practice because the exact solution of the coarse grid equation is required. The system on the coarse grid is easier to solve than the one on the fine grid. By choosing a coarse grid size $H = 2h$ and uniform refinement, the number of unknowns decreases about to an half (in one dimension). In practical applications we are interested in solving fine grid equations with millions of unknowns, therefore, the coarse grid equation has still a too large complexity, such that the overall two-grid method is not optimal with respect to the computational effort. They serve only as the (theoretical) basis for the real multigrid method.

The multigrid idea starts from the observation that in a convergent two-grid method it is not necessary to solve the coarse grid defect equation (2.19) exactly. Instead, without essential loss of convergence speed, one may replace $\underline{v}_H$ by a suitable approximation. A natural way to obtain such an approximation is to apply an analogous two-grid method to (2.19) also, where an even coarser grid than Ω_H is used. Clearly, if the convergence factor of this two-grid method is small enough, it is sufficient to preform only a few, say γ iteration steps to obtain a good enough approximation to the solution of (2.19). This idea can, in a straightforward manner, be applied recursively, using coarser and coarser grids, down to some coarsest grid. On this coarsest grid any solution method can be used (e.g. a direct method or an iterative method if it has sufficiently good convergence properties on the coarsest grid).

The recursive multigrid method (MGM) on level l is then given by the algorithm below. The sequence of operations during one step of the multigrid iteration for $\gamma = 1$ and $\gamma = 2$ is depicted in Figure 2.1. Here $\circ$, $\square$, $\searrow$ and $\nearrow$ mean smoothing, solving exactly, fine-to-coarse and coarse-to-fine transfer, respectively. Due to the Figure 2.1 the cases with $\gamma = 1$ and $\gamma = 2$ are called *V-cycle* and *W-cycle* respectively.

Multigrid method $\texttt{MGM}(l, u, f)$

```
if l = 0 then
   u := K_0^{-1} f  // exact solve on coarsest level
else
   u := S_l^{ν1}(u, f);  //presmoothing step
   d := I_l^{l-1}(K_l u − f);  //restriction of the defect
   v := 0;  //starting value
   for j := 1, ..., γ, do
      MGM(l − 1, v, d)  // solve K_{l−1} v_{l−1} = d_{l−1} by applying γ step of MGM(l − 1, v, d)
   end for
   u := u − I_{l−1}^l v  //update on level l
   u := S_l^{ν2}(u, f)  //postsmoothing step
end if
```

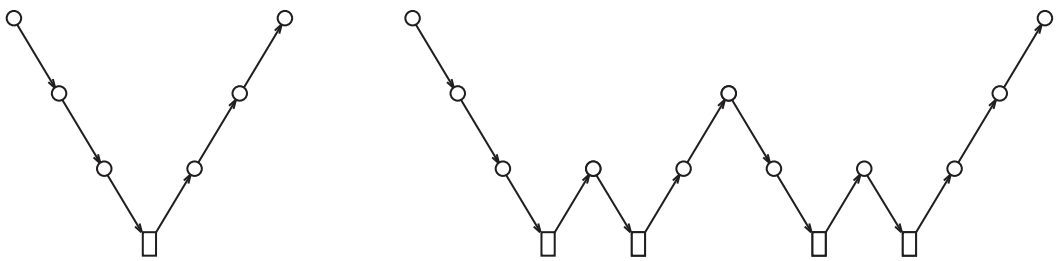

Figure 2.1: V-cycle and W-cycle

Chapter 3

Fourier Analysis and Local Fourier Analysis

In this chapter, we show how *rigorous Fourier analysis* and *local Fourier analysis* (LFA) can be used to derive two-grid convergence factors. The purpose of this chapter is two-fold: first, we want to introduce the idea of rigorous Fourier analysis and LFA and to explain their structures, respectively. Secondly, we want to compute the exact two-grid convergence rate for one-dimensional model problem first by rigorous Fourier analysis and then by LFA.

3.1 Fourier Analysis

3.1.1 Asymptotic Two-Grid Convergence

In the motivation of multigrid method in Section 2.1, we have already studied the smoothing rate of ω-Jacobi iteration using some facts that are characteristic for the rigorous Fourier analysis. We again start with $\varphi_h^k\,(k = 1, \ldots, n-1)$ from (2.7), the discrete eigenfunctions of K_h. The vectors $\{\varphi_h^k : 1 \le k \le n-1\}$ form an orthonormal basis of $\mathbb{R}^{n-1}$, since

$$(\varphi_h^k, \varphi_h^l)_{l^2} = \sum_{j=1}^{n-1} \sqrt{2h}\sin(k\pi jh)\sqrt{2h}\sin(l\pi jh) = \delta_{k,l} \quad 1 \le k, l \le n-1$$

Therefore,the matrix Q_h built by φ_h^k as columns is unitary: $Q_h^{-1} = Q_h^T$,

$$Q_h = [\varphi_h^1, \varphi_h^{n-1}, \varphi_h^2, \varphi_h^{n-2}, \ldots, \varphi_h^k, \varphi_h^{n-k}, \ldots, \varphi_h^{(n/2)-1}, \varphi_h^{(n/2)+1}, \varphi_h^{n/2}] \tag{3.1}$$

Since multiplication by Q_h or Q_h^{-1} does not change the spectral radius, we have

$$\rho(\hat{M}_h^{TGM}) = \rho(M_h^{TGM}) \quad \text{for } \hat{M}_h^{TGM} := Q_h^{-1} M_h^{TGM} Q_h. \tag{3.2}$$

We will show that the Fourier-transformed iteration matrix $Q_h^{-1} M_h^{TGM} Q_h$ of the two-grid method is a block-diagonal matrix of the form

$$\hat{M}_h^{TGM} = \begin{bmatrix} M_h^{(1)} & & & & \\ & M_h^{(2)} & & & \\ & & \ddots & & \\ & & & M_h^{(n/2-1)} & \\ & & & & M_h^{(n/2)} \end{bmatrix} \tag{3.3}$$

with

$$M_h^{(k)} \ (2 \times 2) - \text{matrices} \ \text{ for } 1 \le k \le n/2 - 1, \ M_h^{(n/2)} \ (1 \times 1) - \text{matrix}. \tag{3.4}$$

Thus the determination of the spectral radius $\rho(M_h^{TGM})$ can be reduced to the calculation of the spectral radii of (at most) (2×2)-matrices:

$$\rho(M_h^{TGM}) = \rho(\hat{M}_h^{TGM}) = \max\{\rho(M_h^{(k)}) : 1 \le k \le n/2\}. \tag{3.5}$$

For the proof of the block structure (3.3)-(3.4), we transform the iteration matrix

$$M_h^{TGM} = S_h^{\nu_2} M_h^{CGC} S_h^{\nu_1} \ \text{ with } \ S_h = I - \frac{\omega h}{2} K_h, \ M_h^{CGC} = I - I_H^h K_H^{-1} I_h^H K_h. \tag{3.6}$$

into

$$\hat{M}_h^{TGM} = \hat{S}_h^{\nu_2} (I - \hat{I}_H^h \hat{K}_H^{-1} \hat{I}_h^H \hat{K}_h) \hat{S}_h^{\nu_1} \ \text{ with } \ \hat{K}_h := Q_h^{-1} K_h Q_h, \hat{S}_h := Q_h^{-1} S_h Q_h. \tag{3.7}$$

To define the quantities

$$\hat{I}_H^h := Q_h^{-1} I_H^h Q_H, \quad \hat{K}_H := Q_H^{-1} K_H Q_H, \quad \hat{I}_h^H := Q_H^{-1} I_h^H Q_h, \tag{3.8}$$

we have to introduce the Fourier transformation Q_H at level H. Replacing h in (2.7) by $H = 2h$, we obtain the eigenfunctions of K_H:

$$\varphi_H^k = (\sqrt{4h} \sin(2kj\pi h))_{j=1}^{n/2-1} \quad k = 1, ..., n/2 - 1. \tag{3.9}$$

Analogously to (3.1), the vectors φ_H^k form the matrix

$$Q_H = [\varphi_H^1, \varphi_H^2, \ldots, \varphi_H^{n/2-1}]. \tag{3.10}$$

According to (2.7)-(2.8), $K_h \varphi_h^k = \lambda_h^k \varphi_h^k$ holds with $\lambda_h^k = \frac{4}{h} \sin^2(\frac{1}{2} k\pi h)$. We introduce

$$s_k^2 = \sin^2(\frac{1}{2} k\pi h), \quad c_k^2 = \cos^2(\frac{1}{2} k\pi h). \tag{3.11}$$

Noting that $\lambda_h^{n-k} = \frac{4}{h}s_{n-k}^2 = \frac{4}{h}c_k^2$, we obtain

$$\hat{K}_h := Q_h^{-1} K_h Q_h = \begin{bmatrix} K_h^{(1)} & & & \\ & K_h^{(2)} & & \\ & & \ddots & \\ & & & K_h^{(n/2)} \end{bmatrix} \tag{3.12}$$

with the blocks

$$K_h^{(k)} = \frac{4}{h}\begin{bmatrix} s_k^2 & 0 \\ 0 & c_k^2 \end{bmatrix} \quad \text{for } 1 \le k \le n/2-1, \quad K_h^{(n/2)} = \frac{2}{h}. \tag{3.13}$$

For S_h we have

$$\begin{aligned} S_h\varphi_h^k &= (1-2\omega s_k^2)\varphi_h^k, \\ S_h\varphi_h^{n-k} &= (1-2\omega c_k^2)\varphi_h^{n-k}. \end{aligned}$$

Thus, we obtain

$$\hat{S}_h := Q_h^{-1} S_h Q_h = \begin{bmatrix} S_h^{(1)} & & & \\ & S_h^{(2)} & & \\ & & \ddots & \\ & & & S_h^{(n/2)} \end{bmatrix} \tag{3.14}$$

with the blocks

$$S_h^{(k)} = \begin{bmatrix} 1-2\omega s_k^2 & 0 \\ 0 & 1-2\omega c_k^2 \end{bmatrix} \quad \text{for } 1 \le k \le n/2-1, \quad S_h^{(n/2)} = 1-\omega. \tag{3.15}$$

Since $K_H\varphi_H^k = \lambda_H^k\varphi_H^k$ with $\lambda_H^k = \frac{4}{2h}\sin^2(\frac{1}{2}k\pi 2h) = \frac{2}{h}\sin^2(k\pi h)$ and $\sin^2(k\pi h) = 4s_k^2c_k^2$, we obtain the diagonal matrix

$$\hat{K}_H := Q_H^{-1} K_H Q_H = \operatorname{diag}\{K_H^{(1)}, \ldots, K_H^{(n/2-1)}\} \quad \text{with} \quad K_H^{(k)} = \frac{8}{h}s_k^2c_k^2. \tag{3.16}$$

Next, we study the transfer operators I_h^H and I_H^h defined by (2.21) and (2.24) respectively. From the definition of I_h^H:

$$I_h^H u_h(x) = \frac{1}{2}u_h(x-h) + u_h(x) + \frac{1}{2}u_h(x+h), \quad \text{for } x \in \Omega_H$$

we get

$$\begin{aligned} I_h^H \sin(k\pi x) &= [\sin(k\pi(x-h)) + 2\sin(k\pi x) + \sin(k\pi(x+h))]/2 \\ &= [1+\cos(k\pi h)]\sin(k\pi x) \\ &= 2\cos^2(\frac{1}{2}k\pi h)\sin(k\pi x) \\ &= 2c_k^2\sin(k\pi x) \qquad \text{for } x \in \Omega_H \end{aligned}$$

Thus,

$$I_h^H \varphi_h^k = \sqrt{2} c_k^2 \varphi_H^k. \tag{3.17}$$

Since this identity holds for all k, we replace k by $n-k$:

$$I_h^H \varphi_h^{n-k} = \sqrt{2} c_{n-k}^2 \varphi_H^{n-k} = \sqrt{2} s_k^2 \varphi_H^{n-k}.$$

For $0 \le k \le n/2$, the equality $\sin(2kj\pi h) = -\sin(2(n-k)j\pi h)$ leads to

$$\varphi_H^{n-k} = -\varphi_H^k.$$

Then, we get

$$I_h^H \varphi_h^{n-k} = -\sqrt{2} s_k^2 \varphi_H^k. \tag{3.18}$$

From (3.17) and (3.18) we obtain the representation

$$\hat{I}_h^H := Q_H^{-1} I_h^H Q_h = \begin{bmatrix} r^{(1)} & & & & 0 \\ & r^{(2)} & & & 0 \\ & & \ddots & & \vdots \\ & & & r^{(n/2-1)} & 0 \end{bmatrix} \tag{3.19}$$

with

$$r^{(k)} = \sqrt{2} \begin{bmatrix} c_k^2, & -s_k^2 \end{bmatrix}. \tag{3.20}$$

This means that the last column of $\hat{I}_h^H$ vanishes (this follows from $I_h^H \varphi_h^{n/2} = 0$) and that the remaining part of the format $(n/2-1) \times (n-2)$ consists of $n/2-1$ (1×2)-blocks $r^{(k)}$.

I_H^h from (2.21) and I_h^H from (2.24) are connected by $I_H^h = (I_h^H)^T$, thus, we derive the representation

$$\hat{I}_H^h := Q_h^{-1} I_H^h Q_H = Q_h^{-1} (I_h^H)^T Q_H = Q_h^T (I_h^H)^T Q_H = (Q_H^T I_h^H Q_h)^T = (\hat{I}_h^H)^T. \tag{3.21}$$

From (3.19) we obtain

$$\hat{I}_H^h := Q_h^{-1} I_H^h Q_H = \begin{bmatrix} p^{(1)} & & & \\ & p^{(2)} & & \\ & & \ddots & \\ & & & p^{(n/2-1)} \\ 0 & 0 & \cdots & 0 \end{bmatrix} \tag{3.22}$$

with

$$p^{(k)} = \sqrt{2} \begin{bmatrix} c_k^2 \\ -s_k^2 \end{bmatrix}. \tag{3.23}$$

Since all factors in (3.6) have a block-diagonal structure, this carries over to M_h^{TGM} and proves the structure (3.3)-(3.4). For the (2×2) blocks $M_h^{(k)} (1 \le k \le n/2-1)$ and the 1×1 block $M_h^{n/2}$, the relations (3.13), (3.15), (3.16), (3.20) and (3.23) yield

$$\begin{aligned} M_h^{(k)} &= (S_h^{(k)})^{\nu_2}(I - p^{(k)}(K_H^{(k)})^{-1}r^{(k)}K_h^{(k)})(S_h^{(k)})^{\nu_1} \quad (1 \le k \le n/2-1), \\ M_h^{(n/2)} &= (1-\omega)^{\nu_1+\nu_2}. \end{aligned} \tag{3.24}$$

Inserting the representations of $p^{(k)}, K_H^{(k)}, r^{(k)}, K_h^{(k)}$ and $S_h^{(k)}$, we obtain

$$\begin{aligned} M_h^{(k)} &= \left(S_h^{(k)}\right)^{\nu_2}\left(\begin{bmatrix} 1 & 0 \\ 0 & 1 \end{bmatrix} - \sqrt{2}\begin{bmatrix} c_k^2 \\ s_k^2 \end{bmatrix}\frac{h}{8c_k^2 s_k^2}\sqrt{2}\begin{bmatrix} c_k^2 & -s_k^2 \end{bmatrix}\frac{4}{h}\begin{bmatrix} s_k^2 & 0 \\ 0 & c_k^2 \end{bmatrix}\right)\left(S_h^{(k)}\right)^{\nu_1} \\ &= \left(S_h^{(k)}\right)^{\nu_2}\left(\begin{bmatrix} 1 & 0 \\ 0 & 1 \end{bmatrix} - \begin{bmatrix} c_k^2 & -c_k^2 \\ -s_k^2 & s_k^2 \end{bmatrix}\right)\left(S_h^{(k)}\right)^{\nu_1} \\ &= \begin{bmatrix} 1-2\omega s_k^2 & 0 \\ 0 & 1-2\omega c_k^2 \end{bmatrix}^{\nu_2}\begin{bmatrix} s_k^2 & c_k^2 \\ s_k^2 & c_k^2 \end{bmatrix}\begin{bmatrix} 1-2\omega s_k^2 & 0 \\ 0 & 1-2\omega c_k^2 \end{bmatrix}^{\nu_1}. \end{aligned} \tag{3.25}$$

The block $M_h^{(k)}$ describes the application of M_h^{TGM} to the two functions $\varphi_h^k, \varphi_h^{n-k}$ (respective columns of the matrix Q_h, cf. (3.1)). Since $\rho(AB) = \rho(BA)$ for any linear operators A and B, $\rho(M_h^{TGM}) = \max\{\rho(M_h^{(k)}) : 1 \le k \le n/2\}$ does not depend on ν_1 and ν_2 individually. It depends in particular on the parameter ω and on $\nu = \nu_1 + \nu_2$. In the following, we shall use

$$\rho(h, \nu; \omega) := \rho(M_h^{TGM}(\nu_1, \nu_2; \omega)) \tag{3.26}$$

to denote the convergence factor of two-grid method.
Since for $k = 1, \ldots, n/2-1$,

$$\begin{aligned} \rho(M_h^{(k)}) &= \rho((S_h^{(k)})^{\nu_2}(I - p^{(k)}(K_H^{(k)})^{-1}r^{(k)}K_h^{(k)})(S_h^{(k)})^{\nu_1}) \\ &= \rho((I - p^{(k)}(K_H^{(k)})^{-1}r^{(k)}K_h^{(k)})(S_h^{(k)})^{\nu_2}(S_h^{(k)})^{\nu_1})) \\ &= \rho((I - p^{(k)}(K_H^{(k)})^{-1}r^{(k)}K_h^{(k)})(S_h^{(k)})^{\nu}) \\ &= \rho\left(\begin{bmatrix} s_k^2(1-2\omega s_k^2)^\nu & c_k^2(1-2\omega c_k^2)^\nu \\ s_k^2(1-2\omega s_k^2)^\nu & c_k^2(1-2\omega c_k^2)^\nu \end{bmatrix}\right) \\ &= |s_k^2(1-2\omega s_k^2)^\nu + c_k^2(1-2\omega c_k^2)^\nu| \\ &= |s_k^2(1-2\omega s_k^2)^\nu + (1-s_k^2)(1-2\omega+2\omega s_k^2)^\nu| \\ &= \rho_\nu(s_k^2) \end{aligned} \tag{3.27}$$

and

$$\rho_\nu(\frac{1}{2}) = |(1-\omega)^\nu| = \rho(M_h^{(n/2)})$$

we get

$$\rho(h, \nu; \omega) = \max\{\rho_\nu(s_k^2) : 1 \le k \le n/2\}. \tag{3.28}$$

In practice, we are more interested in the *asymptotic convergence factor*

$$\rho^*(\nu; \omega) := \sup\{\rho(h, \nu; \omega) : h \le 1/2\}. \tag{3.29}$$

In our model problem, we have

$$\rho^*(\nu;\omega) = \sup\{\rho_\nu(s_k^2) : 0 < s_k^2 \le 1/2\}. \tag{3.30}$$

In particular, we study the optimal choices of ω when ν is fixed to be 1 or 2:

- For $\nu = 1$, we have

$$\begin{aligned} \rho_1(s_k^2) &= -4\omega\,(s_k^2 - \frac{1}{2})^2 - \omega + 1, \\ \rho(h;\omega) &= \max\{|1-\omega|, |1-\omega(1+\cos^2\pi h)|\}, \\ \rho^*(\omega) &= \max\{|1-\omega|, |1-2\omega|\}. \end{aligned}$$

  The choice $w = 2/3$ is optimal in the following sense:

$$\inf\{\rho^*(\omega) : 0 \le \omega \le 1\} = \rho^*(\frac{2}{3}) = \frac{1}{3}.$$

  With respect to $\rho(h;\omega)$, we obtain

$$\inf\{\rho(h;\omega) : 0 \le \omega \le 1\} = \rho(h; \frac{2}{2+\cos^2\pi h}) = \frac{\cos^2\pi h}{2+\cos^2\pi h}.$$

- For $\nu = 2$, we obtain from (3.27)

$$\begin{aligned} \rho_2(s_k^2) &= (-8\omega + 12\omega^2)(s_k^2 - \frac{1}{2})^2 + (1-\omega)^2, \\ \rho(h;\omega) &= \max\{(1-\omega)^2, |(3\omega^2 - 2\omega)\cos^2\pi h + (1-\omega)^2|\}, \\ \rho^*(\omega) &= \max\{(1-\omega)^2, (1-2\omega)^2\}. \end{aligned}$$

  The choice $w = 2/3$ is optimal in the following sense:

$$\inf\{\rho^*(\omega) : 0 \le \omega \le 1\} = \rho^*(\frac{2}{3}) = \frac{1}{9}.$$

  With respect to $\rho(h;\omega)$, we obtain

$$\inf\{\rho(h;\omega) : 0 \le \omega \le 1\} = \rho(h; \frac{2}{3}) = \frac{1}{9}.$$

The optimal choices of ω in these two cases are the same with the choice in the smoothing analysis in (2.16). This is a strong indication that $\omega = 2/3$ is a good choice in the multigrid method.

3.1.2 Towards Local Fourier Analysis

Based on rigorous Fourier analysis many results have been obtained for different model problems in 2D and 3D, for different discretizations, coarsening strategies, transfer operators and smoothing procedures, e.g. [21, 22, 23].

As we have seen in the previous section, using rigorous Fourier analysis for an *exact* calculation of the spectral radius of the k-grid operator which are quantitative measures for the error reduction, it is necessary that there exists a unitary basis of periodic eigenfunctions of K_h which generate the whole space of grid functions and which are compatible with the boundary conditions. Then it is possible to expand the error after the i-th k-grid iteration into a Fourier series by a unitary basis transformation, and different multigrid methods can be analyzed by evaluating their effect on the eigenfunctions. The main disadvantages of rigorous Fourier analysis is, however, that it can directly be applied to a rather small class of problems. As soon as we deal with more complicated domains, operators or boundary conditions an appropriate basis of unitary eigenfunctions cannot be derived explicitly. Thus, we will, in general, not be able to apply the rigorous Fourier analysis. The situation is different for the local Fourier analysis (LFA). We will introduce the basic ideas and formalism of LFA in next section.

In this section, we will point out that the rigorous Fourier analysis and the LFA are closely related. The mathematical substance of both is very similar.

The relationship is most easily explained by reconsidering the 1D Poisson equation with *periodic boundary conditions*. Using again finite element discretization and for the corresponding grid Ω_h, the discrete eigenfunctions are

$$\varphi_h^k = e^{i2\pi kx} \quad (k = 0, 1, \ldots, n-1). \tag{3.31}$$

Because of periodicity, we have

$$e^{i2\pi k'x} = e^{i2\pi kx} \quad \text{on } \Omega_h \quad \text{if } k' = k \,(\text{mod } n). \tag{3.32}$$

Shifting k and assuming n to be even, we can thus renumber the eigenfunctions (3.31) as follows

$$0 \le k < n-1 \longleftrightarrow -\frac{n}{2} \le k < \frac{n}{2}. \tag{3.33}$$

This numeration is convenient and is customary in the local Fourier analysis context described in the next section. With the notation

$$\theta := 2\pi\frac{k}{n} = 2\pi kh \tag{3.34}$$

and

$$\Theta_h = \{\theta = 2\pi\frac{k}{n} : -\frac{n}{2} \le k < \frac{n}{2}; k \in \mathbb{Z}\}, \tag{3.35}$$

we can write the discrete eigenfunctions (3.31) in the form

$$\varphi_h(\theta, x) = e^{i\theta x/h} \quad (\theta \in \Theta_h). \tag{3.36}$$

Obviously,

$$\Theta_h \subset [-\pi, \pi), \quad \#\Theta_h = n. \tag{3.37}$$

In case of standard coarsening we can split Θ_h into subsets corresponding to low and high frequencies

$$\begin{aligned} \Theta_h^{low} &:= \{\theta = 2\pi\frac{k}{n} : -\frac{n}{4} \le k < \frac{n}{4}; k \in \mathbb{Z}\} \subset [-\frac{\pi}{2}, \frac{\pi}{2}), \\ \Theta_h^{high} &:= \Theta_h \setminus \Theta_h^{low} \subset [-\pi, \pi) \setminus [-\frac{\pi}{2}, \frac{\pi}{2}). \end{aligned} \tag{3.38}$$

The LFA formalism is based on the grid functions (3.36). However, instead of considering only a finite number of these functions (varying θ in the *finite* set Θ_h), we will allow θ to vary continuously in $[-\pi, \pi)$. This makes the formulation easier and more convenient. Correspondingly, low frequencies θ vary in $[\pi/2, \pi/2)$ and high frequencies vary θ in $[-\pi, \pi) \setminus [\pi/2, \pi/2)$.

Remark 3.1. *For clarification, if all θ vary continuously in $[-\pi, \pi)$, the $\varphi_h(\theta, x)$ no longer fulfill the discrete periodic boundary conditions in $[0, 1]$ (only those φ_h with $\theta \in \Theta_h$ fulfill them). Consequently, we will consider the $\varphi(\theta, \cdot)$ on the infinite grid $G_h := \{x : x = x_j = jh; j \in \mathbb{Z}\}$.*

3.2 Local Fourier Analysis

Local Fourier analysis (or *local mode analysis*) was introduced by Brandt in [6] and developed further in several papers (see [8] and the references given there). This theoretical approach can be regarded from different points of view and has several objectives. We here consider it as a general tool for providing quantitative and realistic insight into the smoothing properties of relaxation methods and the convergence properties of two-grid methods. Our notation is related to the notation and philosophy from [21, 22, 25].

3.2.1 Formal Tools of Local Fourier Analysis

In describing the fundamental ideas of LFA, we confine ourselves to the 1D case and to standard coarsening ($H = 2h$). But it can be immediately carried to d dimensions. The local Fourier analysis is based on certain idealized assumptions and simplifications: the boundary conditions are neglected and the problem is considered on regular infinite grids

$$G_h = \{x : x = x_j = jh; j \in \mathbb{Z}\}. \tag{3.39}$$

On G_h, we consider a discrete operator L_h corresponding to a difference *stencil*

$$L_h \;\hat{=}\; [l_\kappa]_h \quad (\kappa \in \mathbb{Z}) \tag{3.40}$$

$$\text{i.e.} \quad L_h u_h(x) = \sum_{\kappa \in J} l_\kappa u_h(x + \kappa h) \tag{3.41}$$

with constant coefficients $l_\kappa \in \mathbb{R}$ (i.e., l_κ does not depend on x), which, of course, will usually depend on h. Here, $J \subset \mathbb{Z}$ is a certain finite index set defining the so-called difference stencil.

The fundamental quantities in the LFA are the grid functions

$$\varphi(\theta, x) = e^{i\theta x/h} \quad \text{for } x \in G_h. \tag{3.42}$$

We assume that θ varies *continuously* in $\mathbb{R}$. We recognize that

$$\varphi(\theta, x) = \varphi(\theta', x) \quad \text{for } x \in G_h$$

if and only if

$$\theta = \theta' \,(\mathrm{mod}\, 2\pi).$$

Therefore, it is sufficient to consider

$$\varphi(\theta, x) \quad \text{with } \theta \in [-\pi, \pi).$$

The grid functions φ for $-\pi \le \theta < \pi$ are linearly independent on G_h. Obviously, they are all formal eigenfunctions of L_h:

$$L_h\varphi(\theta, x) = \tilde{L}_h(\theta)\varphi(\theta, x) \quad (x \in G_h, \theta \in [-\pi, \pi))$$

with the corresponding eigenvalues or *symbols* of L_h

$$\tilde{L}_h(\theta) = \sum_{\kappa \in J} l_\kappa e^{i\theta \cdot k}. \tag{3.43}$$

In addition to G_h, we assume an infinite coarse grid

$$G_H = \{x : x = x_j = jH; j \in \mathbb{Z}\} \tag{3.44}$$

is obtained by standard coarsening of G_h ($H = 2h$).

For the smoothing and two-grid analysis, we again have to distinguish high and low frequency components on G_h with respect to G_H. The definition is based on the fact that only those frequency components

$$\varphi(\theta, \cdot) \quad \text{with} \quad -\frac{\pi}{2} \le \theta < \frac{\pi}{2}$$

are distinguishable on G_H. For each $\theta' \in [-\pi/2, \pi/2)$, the other frequency component $\varphi(\theta, \cdot)$ with $\theta \in [-\pi, \pi) \setminus [-\pi/2, \pi/2)$ coincide on G_H with $\varphi(\theta', \cdot)$ and are not distinguishable (*not visible*) on G_H. Actually, we have

$$\varphi(\theta, x) = \varphi(\theta', x) \quad \text{for } x \in G_H \quad \text{if and only if} \quad \theta = \theta' \,(\mathrm{mod}\ \pi). \tag{3.45}$$

This leads to the following definition.

Definition 3.2. (high and low frequencies for standard coarsening)

$$\begin{aligned} \varphi \text{ low frequency component} &\iff \theta \in \Theta^{low} := [-\frac{\pi}{2}, \frac{\pi}{2}) \\ \varphi \text{ high frequency component} &\iff \theta \in \Theta^{high} := [-\pi, \pi) \setminus [-\frac{\pi}{2}, \frac{\pi}{2}) \end{aligned} \tag{3.46}$$

This definition is analogous to (2.13) and (3.38), respectively. In addition to speaking of high and low frequency components $\varphi(\theta, \cdot)$, we will, for simplicity, sometimes call the corresponding θs high frequency or low frequency.

3.2.2 Smoothing Analysis

According to Definition 3.2, we distinguish high and low frequency components $\varphi(\theta,\cdot)$ and define the smoothing factor $\mu_{loc}(S_h)$ by

Definition 3.3.

$$\mu_{loc} = \mu_{loc}(S_h) := \sup\{|\tilde{S}_h(\theta)| : \theta \in \Theta^{high}\}. \tag{3.47}$$

To calculate the smoothing factor for our model problem, we have to compute the symbol of the smoothing operator

$$S_h\varphi(\theta,x) = \tilde{S}_h\varphi(\theta,x) \quad (-\pi \le \theta < \pi). \tag{3.48}$$

Inserting (2.6), we obtain

$$S_h\varphi(\theta,x) = (I - \frac{\omega h}{2}K_h)\varphi(\theta,x) = (\tilde{I} - \frac{\omega h}{2}\tilde{K}_h)\varphi(\theta,x).$$

Thus,

$$\tilde{S}_h = \tilde{I} - \frac{\omega h}{2}\tilde{K}_h \tag{3.49}$$

where $\tilde{I}$ and $\tilde{K}_h$ are the symbols of I and K_h, respectively. Rewriting I and K_h in stencil forms

$$I = [0,1,0]_h, \quad K_h = \frac{1}{h}[-1,2,-1]_h. \tag{3.50}$$

From (3.43), we get

$$\tilde{I} = 1, \quad \tilde{K}_h = \frac{1}{h}(2 - 2\cos\theta). \tag{3.51}$$

According to (3.49) and (3.51), the symbol $\tilde{S}_h(\theta)$ is

$$\tilde{S}_h(\theta) = 1 - \omega(1 - \cos\theta). \tag{3.52}$$

For the smoothing factor, we obtain

$$\mu_{loc}(S_h(\omega)) = \max\{|1-\omega|, |1-2\omega|\}. \tag{3.53}$$

This is the same result that we obtained in Section 2.1.3 for $\mu^*(\omega)$. So, ω-Jacobi for symmetric operators can be treated by both rigorous Fourier analysis and LFA. The results are the same, apart from the following slight formal difference: in comparison with (2.15), we recognize that the h-dependence of $\mu(S_h(\omega))$ has disappeared here. This is due to the fact that θ varies continuously in Θ^{high}.

3.2.3 Two-grid Analysis

Let us now apply LFA to the two-grid operator (3.6)

$$M_h^{TGM} = S_h^{\nu_2} M_h^{CGC} S_h^{\nu_1} \quad \text{with} \quad M_h^{CGC} = I - I_H^h K_H^{-1} I_h^H K_h.$$

In order to calculate convergence factors of M_h^{TGM}, we will analyze how the operators K_h, I_h^H, K_H, I_H^h and S_h act on the Fourier components $\varphi(\theta, \cdot)$. The analysis uses the fact that doubles of the $\varphi(\theta, \cdot)$ coincide on G_H. For any low frequency $\theta \in \Theta^{low} = [-\pi/2, \pi/2)$, we consider the frequencies

$$\theta^0, \quad \theta^1$$

where

$$\theta^1 := \begin{cases} \theta^0 + \pi & \text{if } \theta^0 < 0 \\ \theta^0 - \pi & \text{if } \theta^0 > 0 \end{cases} \tag{3.54}$$

As mentioned in (3.45), for any low frequency the above defined frequencies coincide on the coarse grid. Interpreting the Fourier components as coarse-grid functions gives

$$\varphi_h(\theta^0, x) = \varphi_{2h}(2\theta^0, x) = \varphi_{2h}(2\theta^1, x) \quad \text{with} \quad \theta^0 \in \Theta^{low}, x \in G_{2h}. \tag{3.55}$$

Definition 3.4. (harmonics for standard coarsening)
The corresponding two $\varphi(\theta^\alpha, \cdot)$ (and sometimes also the corresponding frequencies) θ^α are called harmonics (of each other). For a given $\theta = \theta^0 \in \Theta^{low}$, we define its *two-dimensional space of harmonics* by

$$E_h^\theta := \text{span}[\varphi(\theta^\alpha, \cdot) : \alpha \in \{0, 1\}]. \tag{3.56}$$

It will turn out below that the two-grid operator M_h^{TGM} leaves the spaces E_h^θ invariant yielding a simple block-diagonal representation for M_h^{TGM} consisting of (2×2)-blocks

$$M_h^{TGM} \mid_{E_h^\theta} =: \hat{M}_h^{TGM}(\theta) \quad (\theta \in \Theta^{low}) \tag{3.57}$$

where $\hat{M}_h^{TGM}(\theta)$ denotes the representation of the two-grid operator on E_h^θ. The *asymptotic convergence factor* ρ_{loc} is then defined as follows:

$$\rho_{loc}(M_h^{TGM}) = \sup\{\rho(\hat{M}_h^{TGM}) : \theta \in \Theta^{low}\}, \tag{3.58}$$

where $\rho_{loc}(\hat{M}_h^{TGM})$ is the spectral radius of the (2×2)-matrix $\hat{M}_h^{TGM}$.

We will now derive the representation of M_h^{TGM} by (2×2)-matrices by calculating the Fourier representation of each multigrid component with respect to the harmonics E_h^θ separately. For clarity, we now write $2h$ instead of H.

- **Fourier representations of operators K_h and I**
  The treatment of the fine-grid discretization K_h is particularly simple, as the Fourier components are eigenfunctions for constant coefficient operators $K_h \hat{=} [k_\kappa]_h$.

From (3.43) we immediately obtain the Fourier representation of K_h with respect to the harmonics E_h^θ:

$$\hat{K}_h(\theta) = \begin{pmatrix} \tilde{K}_h(\theta^0) & 0 \\ 0 & \tilde{K}_h(\theta^1) \end{pmatrix} \tag{3.59}$$

with Fourier symbols $\tilde{K}_h(\theta^\alpha) = 1/h(2 - 2\cos\theta^\alpha)$.
Trivially, the identity operator I is represented by the (2×2)-identity matrix on E_h^θ.

- **Fourier representation of restriction operator I_h^{2h}**
The transfer operator I_h^{2h} is characterized by a stencil

$$I_h^{2h} \hat{=} [r_\kappa]_h^{2h}, \quad i.e. \; I_h^{2h} u_h(x) = \sum_{\kappa \in J} r_\kappa u_h(x + \kappa h), \quad (x \in G_{2h}). \tag{3.60}$$

We have $x + \kappa h \in G_h$ for $x \in G_{2h}$. For the Fourier components this leads to

$$\begin{aligned} (I_h^{2h} \varphi_h(\theta^\alpha, \cdot))(x) &= \sum_{\kappa \in J} r_\kappa \varphi_h(\theta^\alpha, x + \kappa h) = \sum_{\kappa \in J} r_\kappa e^{i(x+\kappa h)\theta^\alpha / h} \\ &= \sum_{\kappa \in J} r_\kappa e^{i\kappa\theta^\alpha} \varphi_h(\theta^\alpha, x) \\ &= \sum_{\kappa \in J} r_\kappa e^{i\kappa\theta^\alpha} \varphi_{2h}(2\theta^0, x) \quad (x \in G_{2h}) \end{aligned} \tag{3.61}$$

with Fourier symbol

$$\tilde{I}_h^{2h}(\theta^\alpha) := \sum_{\kappa \in J} r_\kappa e^{i\kappa\theta^\alpha} \tag{3.62}$$

The Fourier representation of I_h^{2h} is given by a (1×2)-matrix

$$\hat{I}_h^{2h}(\theta) = [\tilde{I}_h^{2h}(\theta^0), \tilde{I}_h^{2h}(\theta^1)]. \tag{3.63}$$

For the model problem, the Fourier symbol of $I_h^{2h} = [1/2, 1, 1/2]_h^{2h}$ is

$$\tilde{I}_h^{2h}(\theta^\alpha) = 1 + \cos\theta^\alpha. \tag{3.64}$$

- **Fourier representation of prolongation operator I_{2h}^h**
The linear interpolation defined in (2.24) can be expressed in stencil notation

$$I_{2h}^h =]p_\kappa[_{2h}^h =]1/2, 1, 1/2[_{2h}^h \tag{3.65}$$

The stencil elements correspond to weights in a distribution process. Therefore, the brackets are reversed . For example, each coarse-grid value $v_{2h}(x)$ $(x \in G_{2h})$ is distributed to its two neighbors weighted by $p_{-1} = p_1 = 1/2$ to obtain fine-grid values for $(I_{2h}^h v_{2h}(x))(x)$ with $x \in G_h \setminus G_{2h}$.

We now investigate the mapping of coarse-grid Fourier components $\varphi_{2h}(2\theta^0,\cdot)$ onto the fine grid by linear interpolation I_{2h}^h.
Assuming $x \in G_{2h}$ leads to

$$(I_{2h}^h\varphi_{2h}(2\theta^0,\cdot))(x) = \varphi_{2h}(2\theta^0,x) = \varphi_h(\theta^0,x). \tag{3.66}$$

Using $\varphi_{2h}(2\theta^0,x) = \varphi_h(\theta^0,x)$ ($x \in G_{2h}$, $\theta^0 \in \Theta^{low}$) we obtain for $x \in G_h \setminus G_{2h}$

$$\begin{aligned}(I_{2h}^h\varphi_{2h}(2\theta^0,\cdot))(x) &= \frac{1}{2}(\varphi_h(\theta^0,x-h)+\varphi_h(\theta^0,x+h))\\ &= \frac{1}{2}(e^{-i\theta^0}+e^{i\theta^0})\varphi_h(\theta^0,x)\\ &= \cos\theta^0\varphi_h(\theta^0,x).\end{aligned} \tag{3.67}$$

Then we obtain the following mapping of $\varphi_{2h}(2\theta^0,\cdot)$ onto the fine grid:

$$(I_{2h}^h\varphi_{2h}(2\theta^0,\cdot))(x) := \begin{cases}\varphi_h(\theta^0,x) & \text{for } x \in G_{2h}\\ \cos\theta^0\varphi_h(\theta^0,x) & \text{for } x \in G_h \setminus G_{2h}\end{cases} \tag{3.68}$$

For the harmonics, it can be easily established that

$$\varphi_h(\theta^0,x) := \begin{cases}\varphi_h(\theta^1,x) & \text{for } x \in G_{2h}\\ -\varphi_h(\theta^1,x) & \text{for } x \in G_h \setminus G_{2h}\end{cases} \tag{3.69}$$

Furthermore, we introduce two functions $\psi_1(x)$ and $\psi_2(x)$ defined by:

$$\begin{aligned}\psi_1(x) &= \frac{1}{2}(\varphi_h(\theta^0,x)+\varphi_h(\theta^1,x)),\\ \psi_2(x) &= \frac{1}{2}(\varphi_h(\theta^0,x)-\varphi_h(\theta^1,x)).\end{aligned} \tag{3.70}$$

The following relations are valid:

$$\psi_1(x) = \begin{cases}\varphi_h(\theta^0,x) & x \in G_{2h}\\ 0 & x \in G_h \setminus G_{2h},\end{cases} \qquad \psi_2(x) = \begin{cases}0 & x \in G_{2h}\\ \varphi_h(\theta^0,x) & x \in G_h \setminus G_{2h}\end{cases} \tag{3.71}$$

Due to (3.71), (3.68) can be rewritten for an arbitrary $x \in G_h$ as a linear combination of $\varphi_h(\theta^\alpha,x)$:

$$\begin{aligned}&(I_{2h}^h\varphi_{2h}(2\theta^0,\cdot))(x)\\ =\ &\psi_1(x)+\cos\theta^0\psi_2(x)\\ =\ &\frac{1}{2}(1+\cos\theta^0)\varphi_h(\theta^0,x)+\frac{1}{2}(1-\cos\theta^0)\varphi_h(\theta^1,x).\end{aligned} \tag{3.72}$$

The symbol for linear interpolation is

$$\tilde{I}_{2h}^h(\theta^\alpha) = \frac{1}{2}\sum_{\kappa\in J} p_\kappa e^{i\theta^\alpha\cdot\kappa}. \tag{3.73}$$

The Fourier representation of I_{2h}^h is then given by a (2×1)-matrix:

$$\hat{I}_{2h}^h(\theta^0) = \begin{bmatrix}\tilde{I}_{2h}^h(\theta^0)\\ \tilde{I}_{2h}^h(\theta^1)\end{bmatrix} = \frac{1}{2}\begin{bmatrix}1+\cos\theta^0\\ 1-\cos\theta^0\end{bmatrix}. \tag{3.74}$$

- **Fourier representation of coarse-grid discretization** K_{2h}
  The stencil notation of K_{2h} is given by

$$K_{2h} = \frac{1}{2h}[-1, 2, -1]_{2h} \tag{3.75}$$

  For $\theta^0 \in \Theta^{low}$, we thus have

$$K_{2h}\varphi_{2h}(2\theta^0, \cdot) = \tilde{K}_{2h}(2\theta)\varphi_{2h}(2\theta^0, \cdot) \tag{3.76}$$

  with the symbol

$$\tilde{K}_{2h}(2\theta) = \sum_{\kappa \in J} k_{\kappa,2h} e^{i2\theta \cdot k} = \frac{1}{2h}(2 - 2\cos(2\theta^0)). \tag{3.77}$$

- **Fourier representation of smoothing operator** S_h
  From Section 3.2.2 we know all Fourier components $\varphi_h(\theta^0, \cdot)$ are formal eigenfunctions of S_h, and S_h can be represented by the diagonal (2×2)-matrix

$$\hat{S}_h(\theta) = \begin{pmatrix} \tilde{S}_h(\theta^0) & 0 \\ 0 & \tilde{S}_h(\theta^1) \end{pmatrix} \tag{3.78}$$

  with $\tilde{S}_h(\theta^\alpha) = 1 - \omega(1 - \cos\theta^\alpha)$.

Inserting the representations of $\hat{I}$, $\hat{I}_{2h}^h$, $\hat{K}_{2h}$, $\hat{I}_h^{2h}$ and $\hat{K}_h$ and using the fact $\cos\theta = \cos\theta^0 = -\cos\theta^1$ ($\theta = \theta^0 \in \Theta^{low}$) we obtain the representation of coarse grid correction operator M_h^{CGC} on E_h^θ

$$\begin{aligned} \hat{M}_h^{CGC}(\theta) &= \hat{I} - \hat{I}_{2h}^h(\theta)(\hat{K}_{2h}(\theta))^{-1}\hat{I}_h^{2h}(\theta)\hat{K}_h(\theta) \\ &= \begin{bmatrix} 1 & 0 \\ 0 & 1 \end{bmatrix} - \begin{bmatrix} \cos^2\frac{\theta}{2} & \cos^2\frac{\theta}{2} \\ \sin^2\frac{\theta}{2} & \sin^2\frac{\theta}{2} \end{bmatrix} \\ &= \begin{bmatrix} \sin^2\frac{\theta}{2} & \cos^2\frac{\theta}{2} \\ \sin^2\frac{\theta}{2} & \cos^2\frac{\theta}{2} \end{bmatrix}. \end{aligned} \tag{3.79}$$

From the representation of M_h^{TGM}

$$\hat{M}_h^{TGM}(\theta) = \hat{S}_h(\theta)^{\nu_2}\hat{M}_h^{CGC}(\theta)\hat{S}_h(\theta)^{\nu_1} \tag{3.80}$$

we obtain the asymptotic convergence factor

$$\rho_{loc}(\nu; \omega) = \sup\{\rho_\nu(\xi) : 0 < \xi \leq \frac{1}{2}\} \tag{3.81}$$

with

$$\rho_\nu(\xi) = |\xi(1 - 2\omega\xi)^\nu + (1 - \xi)(1 - 2\omega + 2\omega\xi)^\nu|, \quad \xi = \sin^2\frac{\theta}{2}. \tag{3.82}$$

This is the same result that we obtained in Section 3.1.1 for $\rho^*(\nu; \omega)$ (see (3.30)) derived by rigorous Fourier analysis. In comparison with (3.30), we recognize that the h-dependence of $\rho(h, \nu; \omega)$ has disappeared here. This is due to the fact that θ varies continuously.

Chapter 4

Application to an Optimal Control Problem

In this chapter we study the smoothing factor and two-grid convergence properties for an optimal control problem. First we give a short introduction of the optimal control problem which we are going to consider. Then we apply both Fourier analysis and local Fourier analysis to the smoothing step and two-grid iteration. The smoother we present here is proposed by W.Zulehner (private communication).

Let $\Omega = (0,1)$. Let $L^2(\Omega)$ and $H^1(\Omega)$ denote the usual Lebesgue space and Sobolev space, respectively. In this chapter we consider the following elliptic optimal control problem: Find the state $y \in H^1(\Omega)$ and the control $u \in L^2(\Omega)$ such that

$$J(y,u) = \min_{(z,v)\in H^1(\Omega)\times L^2(\Omega)} J(z,v)$$

subject to the state equations

$$\begin{aligned} -z'' &= v \quad \text{in} \quad \Omega \quad , \\ z &= 0 \quad \text{at} \quad \Gamma, \end{aligned}$$

with cost functional

$$J(z,v) = \frac{1}{2} \parallel z - y_d \parallel^2_{L^2(\Omega)} + \frac{\gamma}{2} \parallel v \parallel^2_{L^2(\Omega)}$$

where $y_d \in L^2(\Omega)$ is the desired state and $\gamma > 0$ is the weight of the cost of the control (or simply a regularization parameter).

By introducing the adjoint state $p \in H^1(\Omega)$ we get the following optimality system, see e.g.,[24]:
1. The adjoint state equation:

$$\begin{aligned} -p'' &= -(y - y_d) \quad \text{in} \quad \Omega, \\ p &= 0 \qquad\quad\;\; \text{at} \quad \Gamma. \end{aligned} \tag{4.1}$$

2. The control equation:

$$\gamma u - p = 0 \quad \text{in} \quad \Omega. \tag{4.2}$$

3. The state equation:

$$\begin{aligned} -y'' &= u \quad \text{in} \quad \Omega, \\ y &= 0 \quad \text{at} \quad \Gamma. \end{aligned} \tag{4.3}$$

First we use the control equation (4.2) to eliminate the control u. The reduced optimality system consists of two PDEs, the adjoint state equation and state equation, where u is replaced by $\gamma^{-1}p$. The weak formulation of this problem leads to the variational problem: Find $(y,p) \in Y \times Q = H_0^1(\Omega) \times H_0^1(\Omega)$ such that

$$\begin{aligned} (y,w)_{L^2(\Omega)} \;+\; & (p,w)_{H^1(\Omega)} &=\; & \langle y_d, w\rangle \quad \text{for all} \quad w \in Y, \\ (y,q)_{H^1(\Omega)} \;-\; & \gamma^{-1}(p,q)_{L^2(\Omega)} &=\; & 0 \qquad\quad \text{for all} \quad q \in Q. \end{aligned}$$

Let $\mathcal{T}_h$ be a subdivision of the interval $\Omega = (0,1)$ into subintervals with grid size $h = 1/n$ as in Chapter 1. We consider the following discretization by continuous and piecewise linear finite elements:

$$\begin{aligned} Y_h &= \{w \in C(\bar{\Omega}) : w|_T \in P_1 \text{ for all } T \in \mathcal{T}_h, w(0) = w(1) = 0\} \subset Y = H_0^1(\Omega), \\ Q_h &= \{q \in C(\bar{\Omega}) : \; q|_T \in P_1 \text{ for all } T \in \mathcal{T}_h, \; q(0) = \; q(1) = 0\} \subset Q = H_0^1(\Omega), \end{aligned}$$

where P_1 denotes the polynomials of total degree less or equal to 1. Then we obtain the following discrete variational problem: Find $y_h \in Y_h$ and $p_h \in Q_h$ such that

$$\begin{aligned} (y_h,w)_{L^2(\Omega)} \;+\; & (p_h,w)_{H^1(\Omega)} &=\; & \langle y_d, w\rangle \quad \text{for all} \quad w \in Y, \\ (y_h,q)_{H^1(\Omega)} \;-\; & \gamma^{-1}(p_h,q)_{L^2(\Omega)} &=\; & 0 \qquad\quad \text{for all} \quad q \in Q. \end{aligned} \tag{4.4}$$

Finally, by introducing the standard nodal basis, we obtain the following saddle point problem in matrix-vector notation:

$$\mathcal{A}_h \begin{pmatrix} \underline{y}_h \\ \underline{p}_h \end{pmatrix} = \begin{pmatrix} \underline{f}_h \\ 0 \end{pmatrix} \quad \text{with} \quad \mathcal{A}_h = \begin{pmatrix} M_h & K_h \\ K_h & -\frac{1}{\gamma} M_h \end{pmatrix}, \tag{4.5}$$

where K_h denotes the stiffness matrix representing the $H^1(\Omega)$ scalar product on Y_h. It is the same as in (2.3). M_h denotes the mass matrix representing the $L^2(\Omega)$ scalar product on Y_h:

$$M_h = \frac{h}{6} \begin{bmatrix} 4 & 1 & & & \\ 1 & 4 & 1 & & \\ & 1 & \ddots & \ddots & \\ & & \ddots & \ddots & 1 \\ & & & 1 & 4 \end{bmatrix}_{(n-1)\times(n-1)} \tag{4.6}$$

4.1 Fourier analysis for Smoothing Operator

4.1.1 Smoothing Operator

We analyze the following preconditioned Richardson method for the smoothing step:

$$\begin{pmatrix} y_h^{(j+1)} \\ p_h^{(j+1)} \end{pmatrix} = \begin{pmatrix} y_h^{(j)} \\ p_h^{(j)} \end{pmatrix} + \tau \hat{\mathcal{A}}_h^{-1} \left[\begin{pmatrix} f_h \\ 0 \end{pmatrix} - \mathcal{A}_h \begin{pmatrix} y_h^{(j)} \\ p_h^{(j)} \end{pmatrix} \right] \quad \tau \in (0,2) \tag{4.7}$$

where the preconditioner $\hat{\mathcal{A}}_h$ is given by

$$\hat{\mathcal{A}}_h = \begin{pmatrix} M_h & \hat{K}_h \\ \hat{K}_h & -\frac{1}{\gamma} M_h \end{pmatrix} \tag{4.8}$$

with $\hat{K}_h = \alpha \, \mathrm{diag}(K_h)$. The scaling parameter α is chosen small enough to ensure

$$\hat{K}_h \geq K_h. \tag{4.9}$$

In our example, we fix $\alpha = 2$. Then

$$\hat{K}_h = \beta I = \frac{4}{h} I$$

fulfills the assumption (4.9) since $\lambda_{max}(K_h) \leq 4/h$.

The corresponding smoothing operator is

$$\boldsymbol{S}_h = I - \tau \hat{\mathcal{A}}_h^{-1} \mathcal{A}_h. \tag{4.10}$$

This smoother was proposed by W.Zulehner (private communication).

4.1.2 Generalized Eigenvalue Problem

In order to analyze the smoothing properties, we need to know the eigenvalues $\lambda(\boldsymbol{S}_h)$ of the smoothing operator $\boldsymbol{S}_h$. Since

$$\lambda(\boldsymbol{S}_h) = 1 - \tau \lambda(\hat{\mathcal{A}}_h^{-1} \mathcal{A}_h), \tag{4.11}$$

we have to study the generalized eigenvalue problem

$$\mathcal{A}_h x = \chi \hat{\mathcal{A}}_h x. \tag{4.12}$$

This is equivalent to

$$(\mathcal{A}_h - \chi \hat{\mathcal{A}}_h) x = 0. \tag{4.13}$$

Since the two matrices M_h and K_h share the same eigenfunctions

$$\varphi_h^k(M_h) = \varphi_h^k(K_h) = (\sqrt{2h} \sin(kj\pi h))_{j=1}^{n-1} \quad k = 1, ..., n-1, \tag{4.14}$$

we denote

$$P = [\varphi_h^1, \varphi_h^2, \ldots, \varphi_h^{n-2}, \varphi_h^{n-1}]. \tag{4.15}$$

So both M_h and K_h can be diagonalized through similarity transformations:

$$P^{-1} M_h P = \mathrm{diag}\{\lambda_k\}, \quad P^{-1} K_h P = \mathrm{diag}\{\mu_k\} \quad k = 1, ..., n-1, \tag{4.16}$$

where

$$\begin{aligned} \lambda_k &= \lambda_k(M_h) = \frac{h}{3}(2 + \cos(k\pi h)), \\ \mu_k &= \lambda_k(K_h) = \frac{4}{h}\sin^2(\frac{1}{2}k\pi h). \end{aligned} \tag{4.17}$$

Then, we apply the following similarity transformation to the matrix $\mathcal{A}_h - \chi\hat{\mathcal{A}}_h$ and use (4.16)

$$\begin{aligned} & \begin{bmatrix} P^{-1} & 0 \\ 0 & P^{-1} \end{bmatrix} (\mathcal{A}_h - \chi\hat{\mathcal{A}}_h) \begin{bmatrix} P & 0 \\ 0 & P \end{bmatrix} \\ = & \begin{bmatrix} P^{-1} & 0 \\ 0 & P^{-1} \end{bmatrix} \begin{bmatrix} (1-\chi)M_h & K_h - \chi\beta I \\ K_h - \chi\beta I & -\frac{1}{\gamma}(1-\chi)M_h \end{bmatrix} \begin{bmatrix} P & 0 \\ 0 & P \end{bmatrix} \\ = & \begin{bmatrix} (1-\chi)\mathrm{diag}\{\lambda_k\} & \mathrm{diag}\{\mu_k\} - \chi\beta I \\ \mathrm{diag}\{\mu_k\} - \chi\beta I & -\frac{1}{\gamma}(1-\chi)\mathrm{diag}\{\lambda_k\} \end{bmatrix}. \end{aligned} \tag{4.18}$$

We denote

$$a = (1-\chi)\mathrm{diag}\{\lambda_k\}, \quad b = \mathrm{diag}\{\mu_k\} - \chi\beta I, \tag{4.19}$$

then the generalized eigenvalue problem (4.12) reduces to the solution of

$$\det\left(\begin{bmatrix} a & b \\ b & -\frac{1}{\gamma}a \end{bmatrix}\right) = 0. \tag{4.20}$$

It can be easily proved that $\chi = 1$ is not an eigenvalue of (4.18), which means a is nonsingular, then from (4.20) we get

$$\det\left(\begin{bmatrix} a & b \\ 0 & -\frac{1}{\gamma}a - ba^{-1}b \end{bmatrix}\right) = 0,$$

which is equivalent to

$$\det(-\frac{1}{\gamma}a - ba^{-1}b) = 0. \tag{4.21}$$

Inserting (4.19) and (4.17) into (4.21) we get the equation

$$-\frac{1}{\gamma}(1-\chi_k)^2\lambda_k^2 + (\mu_k - \beta\chi_k)^2 = 0. \tag{4.22}$$

Solving this equation we finally obtain the eigenvalues of $\hat{\mathcal{A}}_h^{-1}\mathcal{A}_h$:

$$\chi_k = \frac{(\lambda_k^2 + \gamma\beta\mu_k) \pm i\left[\sqrt{\gamma}\beta\lambda_k - \sqrt{\gamma}\mu_k\lambda_k\right]}{\lambda_k^2 + \gamma\beta^2}. \tag{4.23}$$

Then, the eigenvalues of $\boldsymbol{S}_h$ are given by the relation

$$\lambda_k(S) = 1 - \tau\chi_k = \left(1 - \frac{\tau(\lambda_k^2 + \gamma\beta\mu_k)}{\lambda_k^2 + \gamma\beta^2}\right) \pm i\frac{\tau(\sqrt{\gamma}\beta\lambda_k - \sqrt{\gamma}\mu_k\lambda_k)}{\lambda_k^2 + \gamma\beta^2}, \tag{4.24}$$

with $\beta = 4/h$, λ_k and μ_k as in (4.17).

4.1.3 Smoothing Factor

Theorem 4.1. *The asymptotic smoothing factor for the smoother given in (4.10) is*

$$\mu^*(\tau) = \max\left\{|1-\tau|, |1-\frac{\tau}{2}|\right\} \tag{4.25}$$

The choice $\tau_{opt} = 4/3$ is optimal in the following sense:

$$\min_{\tau\in(0,2)} \mu^*(\tau) = \mu^*(\frac{4}{3}) = \frac{1}{3}. \tag{4.26}$$

Proof: From (4.24) we obtain

$$|\lambda_k(S)|^2 = 1 - \frac{(2\tau - \tau^2)\lambda_k^2 + \gamma(2\tau\beta\mu_k - \tau^2\mu_k^2)}{\lambda_k^2 + \gamma\beta^2}. \tag{4.27}$$

We assume

$$|\lambda_k(S)|^2 \le 1 - \delta, \quad \forall\gamma \in (0,\infty),\ k = \frac{n}{2}, \ldots, n-1,\ h \in (0, \frac{1}{2}) \tag{4.28}$$

where $\delta \neq \delta(k,h)$. We will compute δ in the following. For all $h \in (0, 1/2]$, $k \in \{n/2, \ldots, n-1\}$ and $\gamma \in (0,\infty)$, we have

$$\begin{aligned} |\lambda_k(S)|^2 \le 1 - \delta \quad &\Leftrightarrow \quad 1 - \frac{(2\tau - \tau^2)\lambda_k^2 + \gamma(2\tau\beta\mu_k - \tau^2\mu_k^2)}{\lambda_k^2 + \gamma\beta^2} \le 1 - \delta \\ &\Leftrightarrow \quad (2\tau - \tau^2)\lambda_k^2 + \gamma(2\tau\beta\mu_k - \tau^2\mu_k^2) \ge (\lambda_k^2 + \gamma\beta^2)\delta \\ &\Leftrightarrow \quad \lambda_k^2(2\tau - \tau^2 - \delta) + \gamma(2\tau\beta\mu_k - \tau^2\mu_k^2 - \beta^2\delta) \ge 0 \end{aligned}$$

Let

$$I_1 = \lambda_k^2(2\tau - \tau^2 - \delta), \quad I_2 = (2\tau\beta\mu_k - \tau^2\mu_k^2 - \beta^2\delta),$$

thus

$$|\lambda_k(S)|^2 \le 1 - \delta \Leftrightarrow I_1 + \gamma\, I_2 \ge 0, \quad \forall\gamma,\ h,\ k. \tag{4.29}$$

Since $\gamma \in (0, \infty)$, the relation (4.29) is equivalent to $I_1 \geq 0$ and $I_2 \geq 0$. (To see this, we first let $\gamma \to 0$ and obtain $I_1 \geq 0$. Then rewrite (4.29) as $\frac{1}{\gamma} I_1 + I_2 \geq 0$ and let $\gamma \to \infty$ we obtain $I_2 \geq 0$.) In the following, we consider $I_1 \geq 0$ and $I_2 \geq 0$ separately.

$$\begin{aligned} I_1 \geq 0 &\Leftrightarrow \lambda_k^2(2\tau - \tau^2 - \delta) \geq 0 \\ &\Leftrightarrow \delta \leq 2\tau - \tau^2 \end{aligned} \tag{4.30}$$

and

$$I_2 \geq 0 \Leftrightarrow 2\tau\beta\mu_k - \tau^2\mu_k^2 - \beta^2\delta \geq 0 \quad \forall\, h,\, k \tag{4.31}$$

Inserting $\beta = \frac{4}{h}$, $\mu_k = \frac{4}{h}\sin^2(\frac{1}{2}k\pi h) = \frac{2}{h}(1 - \cos k\pi h)$ into (4.31), we obtain

$$\begin{aligned} I_2 \geq 0 &\Leftrightarrow \frac{16}{h}\tau(1 - \cos k\pi h) - \frac{4}{h^2}\tau^2(1 - \cos k\pi h)^2 - \frac{16}{h^2}\delta \geq 0 \\ &\Leftrightarrow -\frac{\tau^2}{4}(1 - \cos k\pi h)^2 + \tau(1 - \cos k\pi h) - \delta \geq 0 \quad \forall h,\, k. \end{aligned} \tag{4.32}$$

We denote

$$f(y) = -\frac{\tau^2}{4}y^2 + \tau\, y - \delta \text{ with } y \in [1, 2), \quad \text{and} \quad y_k = 1 - \cos k\pi h. \tag{4.33}$$

Then

$$I_2 \geq 0 \Leftrightarrow \inf_{h,k} f(y_k) \geq 0 \tag{4.34}$$

Since for $k = n/2, \ldots, n-1$,

$$1 = y_{\frac{1}{2}} \leq \cdots \leq y_{n-1} = 1 + \cos \pi h$$

and $f(y)$ is convex, we have

$$\begin{aligned} \inf_{h,k} f(y_k) &= \inf_h \min_k f(y_k) = \inf_h \min\left\{f(y_{\frac{n}{2}}), f(y_{n-1})\right\} \\ &= \inf_h \min\{-\frac{\tau^2}{4} + \tau - \delta, -\frac{\tau^2}{4}(1 + \cos \pi h)^2 + \tau\,(1 + \cos \pi h) - \delta\} \\ &= \min\left\{-\frac{\tau^2}{4} + \tau - \delta, 2\tau - \tau^2 - \delta\right\} \end{aligned} \tag{4.35}$$

Hence

$$I_1 + \gamma\, I_2 \geq 0 \Leftrightarrow \delta \leq \min\left\{2\tau - \tau^2, -\frac{\tau^2}{4} + \tau\right\}. \tag{4.36}$$

Inserting (4.36) into (4.28) and take supremum over h, we get

$$\sup_{0 \leq h \leq 1/2} \min_{k \in \{n/2, \ldots n-1\}} |\lambda_k(S)|^2 = \max\left\{(1 - \tau)^2, (1 - \frac{\tau}{2})^2\right\}. \tag{4.37}$$

Finally, according to the definition of asymptotic smoothing factor in (2.14), we obtain

$$\mu^*(\tau) = \max\left\{|1 - \tau|, |1 - \frac{\tau}{2}|\right\}.$$

□

Remark 4.2. *The smoothing factor is independent of the regularization parameter γ. This is a strong indication that the multigrid method is additionally robust with respect to the regularization parameter γ. Nevertheless, the theory presented here is not able to show this robustness.*

4.2 Fourier Two-grid Analysis

In Section 3.1.1, we know the matrix Q_h (see (3.1)) is unitary and multiplication by Q_h or Q_h^{-1} does not change the spectral radius. So we transform the matrix M_h^{TGM} by the similarity transformation $Q_h^{-1} M_h^{TGM} Q_h$ and this matrix is much simpler than the original one. Here, we use the same trick. However, instead of multiplication by Q_h^{-1} and Q_h we use the block diagonal matrices

$$\begin{pmatrix} Q_h^{-1} & 0 \\ 0 & Q_h^{-1} \end{pmatrix}, \qquad \begin{pmatrix} Q_h & 0 \\ 0 & Q_h \end{pmatrix}. \tag{4.38}$$

We have

$$\rho(\overline{\boldsymbol{M}_h^{TGM}}) = \rho(\boldsymbol{M}_h^{TGM}) \tag{4.39}$$

for

$$\overline{\boldsymbol{M}_h^{TGM}} = \begin{pmatrix} Q_h^{-1} & 0 \\ 0 & Q_h^{-1} \end{pmatrix} \boldsymbol{M}_h^{TGM} \begin{pmatrix} Q_h & 0 \\ 0 & Q_h \end{pmatrix}. \tag{4.40}$$

From

$$\boldsymbol{M}_h^{TGM} = \boldsymbol{S}_h{}^{\nu_2} \boldsymbol{M}_h^{CGC} \boldsymbol{S}_h{}^{\nu_1}, \tag{4.41}$$

we obtain

$$\overline{\boldsymbol{M}_h^{TGM}} = \overline{\boldsymbol{S}_h{}^{\nu_2}}\, \overline{\boldsymbol{M}_h^{CGC}}\, \overline{\boldsymbol{S}_h{}^{\nu_1}}. \tag{4.42}$$

We separately consider the coarse grid operator $\boldsymbol{M}_h^{CGC}$ and the smoothing operator $\boldsymbol{S}_h$.

1. Coarse grid correction $\boldsymbol{M}_h^{CGC}$:

$$\begin{aligned}
\boldsymbol{M}_h^{CGC} &= \boldsymbol{I} - \boldsymbol{I}_{2h}^h \mathcal{A}_{2h}^{-1} \boldsymbol{I}_h^{2h} \mathcal{A}_h \\
&= \boldsymbol{I} - \begin{pmatrix} I_{2h}^h & 0 \\ 0 & I_{2h}^h \end{pmatrix} \begin{pmatrix} \frac{1}{\gamma} U_{2h}^{-1} M_{2h} & U_{2h}^{-1} K_{2h} \\ U_{2h}^{-1} K_{2h} & -U_{2h}^{-1} M_{2h} \end{pmatrix} \begin{pmatrix} I_h^{2h} & 0 \\ 0 & I_h^{2h} \end{pmatrix} \begin{pmatrix} M_h & K_h \\ K_h & -\frac{1}{\gamma} M_h \end{pmatrix} \\
&= \boldsymbol{I} - \begin{pmatrix} \frac{1}{\gamma} I_{2h}^h U_{2h}^{-1} M_{2h} I_h^{2h} & I_{2h}^h U_{2h}^{-1} K_{2h} I_h^{2h} \\ I_{2h}^h U_{2h}^{-1} K_{2h} I_h^{2h} & -I_{2h}^h U_{2h}^{-1} M_{2h} I_h^{2h} \end{pmatrix} \begin{pmatrix} M_h & K_h \\ K_h & -\frac{1}{\gamma} M_h \end{pmatrix} \\
&= \boldsymbol{I} - \begin{pmatrix} T_{11} & T_{12} \\ T_{21} & T_{22} \end{pmatrix}
\end{aligned} \tag{4.43}$$

where

$$
\begin{aligned}
U_{2h} &= \frac{1}{\gamma} M_{2h}^2 + K_{2h}^2, && (4.44)\\
T_{11} &= \frac{1}{\gamma} I_{2h}^h U_{2h}^{-1} M_{2h} I_h^{2h} M_h + \frac{1}{\gamma} I_{2h}^h U_{2h}^{-1} K_{2h} I_h^{2h} K_h, && (4.45)\\
T_{12} &= \frac{1}{\gamma} (I_{2h}^h U_{2h}^{-1} M_{2h} I_h^{2h} K_h - I_{2h}^h U_{2h}^{-1} K_{2h} I_h^{2h} M_h), && (4.46)\\
T_{21} &= -\gamma\, T_{12}, && (4.47)\\
T_{22} &= T_{11}, && (4.48)
\end{aligned}
$$

and I_{2h}^h and I_h^{2h} are defined as (2.25) and (2.22).
Since

$$
\begin{aligned}
\overline{\boldsymbol{M}_h^{CGC}} &= \begin{pmatrix} Q_h^{-1} & 0 \\ 0 & Q_h^{-1} \end{pmatrix} \boldsymbol{M}_h^{CGC} \begin{pmatrix} Q_h & 0 \\ 0 & Q_h \end{pmatrix} \\
&= \boldsymbol{I} - \begin{pmatrix} Q_h^{-1} T_{11} Q_h & Q_h^{-1} T_{12} Q_h \\ Q_h^{-1} T_{21} Q_h & Q_h^{-1} T_{22} Q_h \end{pmatrix}, && (4.49)
\end{aligned}
$$

we deal with each component separately. We start with the first term in T_{11}:

$$
\begin{aligned}
& Q_h^{-1} \frac{1}{\gamma} I_{2h}^h U_{2h}^{-1} M_{2h} I_h^{2h} M_h Q_h \\
= \;& \frac{1}{\gamma} Q_h^{-1} I_{2h}^h Q_{2h} Q_{2h}^{-1} (U_{2h}^{-1} M_{2h}) Q_{2h} Q_{2h}^{-1} I_h^{2h} Q_h Q_h^{-1} M_h Q_h \\
= \;& \hat{I}_{2h}^h (\frac{1}{\gamma} \Lambda_{2M}^2 + \Lambda_{2K}^2)^{-1} \Lambda_{2M} \hat{I}_h^{2h} \Lambda_M, && (4.50)
\end{aligned}
$$

where $\hat{I}_{2h}^h$ and $\hat{I}_h^{2h}$ are as in(3.22) and (3.19),

$$
\Lambda_{2M} = \text{diag}\,\{\lambda(M_{2h})\}, \quad \Lambda_{2K} = \text{diag}\,\{\lambda(K_{2h})\}, \tag{4.51}
$$

and

$$
\Lambda_M = \text{diag}\,\{\lambda_1(M_h), \lambda_{n-1}(M_h), \ldots, \lambda_{\frac{n}{2}-1}(M_h), \lambda_{\frac{n}{2}+1}(M_h), \lambda_{\frac{n}{2}}(M_h)\}. \tag{4.52}
$$

The other components are treated in the same way. Thus, we obtain the representation of coarse grid operator $\boldsymbol{M}_h^{CGC}$.

2. Smoothing operator $\boldsymbol{S}_h$:

$$
\begin{aligned}
\boldsymbol{S}_h &= I - \tau \hat{\mathcal{A}}_h^{-1} \mathcal{A}_h \\
&= I - \tau \begin{pmatrix} \frac{1}{\gamma} V^{-1} M_h & V^{-1}\beta I \\ V^{-1}\beta I & -V^{-1} M_h \end{pmatrix} \begin{pmatrix} M_h & K_h \\ K_h & -\frac{1}{\gamma} M_h \end{pmatrix} && (4.53)
\end{aligned}
$$

where

$$
V_h = \frac{1}{\gamma} (M_h^2 + \beta^2 I). \tag{4.54}
$$

It is similar as we have done in the previous step to get the representation of smoothing operator $\boldsymbol{S}_h$.

As soon as we obtain the representations for $\boldsymbol{M}_h^{CGC}$ and $\boldsymbol{S}_h$, we then can analyze the properties of two-grid operator according to (4.42).

4.3 Local Fourier Analysis for Smoothing Operator

Local Fourier analysis for systems of q PDEs is similar to the scalar case we analyzed in previous chapter. Here, we are dealing with *vector-valued* Fourier components

$$\boldsymbol{\varphi}_h(\theta,\cdot) := \varphi_h(\theta,\cdot)\cdot\mathbf{I} \qquad \mathbf{I}=(1,\ldots,1)^T\in\mathbb{R}^q \tag{4.55}$$

and the Fourier symbols

$$\widetilde{\boldsymbol{L}}_h(\theta)=\begin{pmatrix} \widetilde{L}_h^{1,1}(\theta) & \cdots & \widetilde{L}_h^{1,q}(\theta)\\ \vdots & \cdots & \vdots \\ \widetilde{L}_h^{q,1}(\theta) & \cdots & \widetilde{L}_h^{q,q}(\theta)\end{pmatrix} \tag{4.56}$$

are given by $(q\times q)$-matrices consisting of scalar Fourier symbols.

To analyze the smoothing operator by local Fourier analysis, we have to compute the symbol of the operator $\boldsymbol{S}_h$

$$\overline{\boldsymbol{S}_h}=\overline{I-\tau\hat{\mathcal{A}}_h^{-1}\mathcal{A}_h}=\overline{I}-\tau(\overline{\hat{\mathcal{A}}_h})^{-1}\overline{\mathcal{A}_h}.$$

Since the discrete operators M_h and K_h can be written in stencil form, the Fourier symbols $\overline{M_h}$ and $\overline{K_h}$ can be easily computed from the stencil form and are given by

$$\begin{aligned}\overline{M_h}(\theta) &= \frac{h}{6}(4+2\cos\theta),\\ \overline{K_h}(\theta) &= \frac{1}{h}(2-2\cos\theta).\end{aligned} \tag{4.57}$$

The Fourier symbols of the remaining discrete operators are just combinations of the two fundamental symbols $\overline{M_h}$ and $\overline{K_h}$. According to (4.56) the symbols of the discrete operators $\mathcal{A}_h$ and $\hat{\mathcal{A}}_h$ are then the following (2×2)-matrices:

$$\overline{\mathcal{A}_h}=\begin{pmatrix}\overline{M_h} & \overline{K_h}\\ \overline{K_h} & -\frac{1}{\gamma}\overline{M_h}\end{pmatrix},\qquad \overline{\hat{\mathcal{A}}_h}=\begin{pmatrix}\overline{M_h} & \frac{4}{h}I\\ \frac{4}{h}I & -\frac{1}{\gamma}\overline{M_h}\end{pmatrix}. \tag{4.58}$$

Now any symbolic package (such as MAPLE) can be used to compute the symbol of $I-\tau\hat{\mathcal{A}}_h^{-1}\mathcal{A}_h$:

$$\overline{\boldsymbol{S}_h}(\theta)=[s(i,j)]_{i,j=1}^2 \tag{4.59}$$

with

$$s(1,1)=s(2,2)=1-\tau\,\frac{4h^4\cos\theta+h^4\cos^2\theta+72\gamma-72\gamma\cos\theta}{4h^4+4h^4\cos\theta+h^4\cos^2\theta+144\gamma},$$

$$s(2,1) = -\gamma\, s(1,2) = -\gamma\, \frac{6\tau h^2(\cos^2\theta + 3\cos\theta + 2)}{4h^4 + 4h^4\cos\theta + h^4\cos^2\theta + 144\gamma}.$$

and the eigenvalues of this matrix. In the limit case $h \to 0$ we finally obtain for the eigenvalues of $\overline{\boldsymbol{S}_h}$:

$$\lambda_1 = \lambda_2 = 1 - \frac{\tau}{2}(1 - \cos\theta) \tag{4.60}$$

The smoothing factor μ_{loc} is then given by

$$\mu_{loc}(\tau) = \max\{|1-\tau|, |1-\frac{\tau}{2}|\}. \tag{4.61}$$

In order to obtain the best smoothing properties, the term $\mu_{loc}(\tau)$ has to be minimized over the admissible range of the relaxation parameter τ:

$$\min_{\tau\in(0,2)} \mu_{loc}(\tau) = \mu_{loc}(\tau_{opt}) = \frac{1}{3}, \quad \text{with} \quad \tau_{opt} = \frac{4}{3}. \tag{4.62}$$

This is the same result that we obtained in Section 4.1.3 using rigorous Fourier analysis.

4.4 Local Fourier Two-grid Analysis

Local Fourier two-grid analysis for systems of equations is based on the vector-valued Fourier components $\boldsymbol{\varphi}_h(\theta,\cdot)$ introduced in Section 4.3 and the corresponding spaces of harmonics, $\boldsymbol{E}_h^\theta$ with $\theta \in \Theta^{low}$, which are defined analogously to Definition 3.4, replacing the scalar Fourier components by its vector-valued counterparts.

Similar as we treat the model problem, we will derive the representation of $\boldsymbol{M}_h^{TGM}$ by (4×4)-matrices by considering each multigrid component separately,

$$\boldsymbol{M}_h^{TGM}(\theta) = (\boldsymbol{S}_h(\theta))^{\nu_2}\boldsymbol{M}_h^{CGC}(\theta)(\boldsymbol{S}_h(\theta))^{\nu_1} \tag{4.63}$$

with the representation of coarse-grid correction operator $\boldsymbol{M}_h^{CGC}$

$$\boldsymbol{M}_h^{CGC}(\theta) = \boldsymbol{I} - \boldsymbol{I}_{2h}^h(\theta)\mathcal{A}_{2h}^{-1}(\theta)\boldsymbol{I}_h^{2h}(\theta)\mathcal{A}_h(\theta). \tag{4.64}$$

- **Fourier representations of operators $\mathcal{A}_h$ and $\boldsymbol{I}$:**

  $$\mathcal{A}_h(\theta) = \mathrm{bdiag}\{\overline{\mathcal{A}_h}(\theta^0), \overline{\mathcal{A}_h}(\theta^1)\}$$

  Inserting the symbols $\overline{\mathcal{A}_h}$ from (4.58) we obtain the Fourier representation of $\mathcal{A}_h$:

  $$\mathcal{A}_h(\theta) = \begin{bmatrix} \overline{M_h}(\theta^0) & \overline{K_h}(\theta^0) & 0 & 0 \\ \overline{K_h}(\theta^0) & -\frac{1}{\gamma}\overline{M_h}(\theta^0) & 0 & 0 \\ 0 & 0 & \overline{M_h}(\theta^1) & \overline{K_h}(\theta^1) \\ 0 & 0 & \overline{K_h}(\theta^1) & -\frac{1}{\gamma}\overline{M_h}(\theta^1) \end{bmatrix} \tag{4.65}$$

  with $\overline{M_h}(\theta^\alpha)$ and $\overline{K_h}(\theta^\alpha)$ given by (4.57).
  For identity operator, the representation is

  $$\boldsymbol{I} = \mathrm{diag}\{1,\ldots,1\} \in \mathbb{C}^{4\times 4}. \tag{4.66}$$

- **Fourier representation of restriction operator $\boldsymbol{I}_h^{2h}$:**

$$\boldsymbol{I}_h^{2h}(\theta) = \left(\overline{\boldsymbol{I}_h^{2h}}(\theta^0), \overline{\boldsymbol{I}_h^{2h}}(\theta^1)\right) = \begin{bmatrix} \tilde{I}_h^{2h}(\theta^0) & 0 & \tilde{I}_h^{2h}(\theta^1) & 0 \\ 0 & \tilde{I}_h^{2h}(\theta^0) & 0 & \tilde{I}_h^{2h}(\theta^1) \end{bmatrix} \tag{4.67}$$

The Fourier symbols of the restriction operator in connection with systems of equations are given by (2×2)-matrices, similar as for the discretization operators (see (4.56)). They are composed of *scalar* Fourier symbols

$$\overline{\boldsymbol{I}_h^{2h}}(\theta^\alpha) = \begin{bmatrix} \tilde{I}_h^{2h}(\theta^\alpha) & 0 \\ 0 & \tilde{I}_h^{2h}(\theta^\alpha) \end{bmatrix} \tag{4.68}$$

with $\tilde{I}_h^{2h}(\theta^\alpha)$ as in (3.62).

- **Fourier representation of prolongation operator $\boldsymbol{I}_{2h}^h$:**

$$\boldsymbol{I}_{2h}^h(\theta) = \begin{bmatrix} \overline{\boldsymbol{I}_{2h}^h}(\theta^0) \\ \overline{\boldsymbol{I}_{2h}^h}(\theta^1) \end{bmatrix} = \begin{bmatrix} \tilde{I}_{2h}^h(\theta^0) & 0 \\ 0 & \tilde{I}_{2h}^h(\theta^0) \\ \tilde{I}_{2h}^h(\theta^0) & 0 \\ 0 & \tilde{I}_{2h}^h(\theta^1) \end{bmatrix}. \tag{4.69}$$

The Fourier symbols are given by the following (2×2)-matrices

$$\overline{\boldsymbol{I}_{2h}^h}(\theta^\alpha) = \begin{bmatrix} \tilde{I}_{2h}^h(\theta^\alpha) & 0 \\ 0 & \tilde{I}_{2h}^h(\theta^\alpha) \end{bmatrix}, \tag{4.70}$$

where $\tilde{I}_{2h}^h(\theta^\alpha)$ is the same as in (3.73).

- **Fourier representation of coarse-grid discretization $\mathcal{A}_{2h}$:**

$$\mathcal{A}_{2h}(\theta) = \overline{\mathcal{A}_{2h}}(2\theta) = \begin{bmatrix} \overline{M_{2h}}(2\theta) & \overline{K_{2h}}(2\theta) \\ \overline{K_{2h}}(2\theta) & -\frac{1}{\gamma}\overline{M_{2h}}(2\theta) \end{bmatrix}, \tag{4.71}$$

with the symbols of K_{2h} and M_{2h} given by

$$\begin{aligned} \overline{K_{2h}}(2\theta) &= \frac{1}{2h}(2 - 2\cos(2\theta^0)), \text{ and} \\ \overline{M_{2h}}(2\theta) &= \frac{2h}{6}(4 + 2\cos(2\theta^0)). \end{aligned} \tag{4.72}$$

- **Fourier representation of smoothing operator $\boldsymbol{S}_h$:**

$$\boldsymbol{S}_h(\theta) = \text{bdiag}\{\overline{\boldsymbol{S}_h}(\theta^0), \overline{\boldsymbol{S}_h}(\theta^1)\} \in \mathbb{C}^{4\times 4} \tag{4.73}$$

with Fourier symbol $\overline{\boldsymbol{S}_h}(\theta^\alpha)$ given in (4.59).

Inserting the representations of $\mathcal{A}_h$, $\boldsymbol{I}$, $\boldsymbol{I}_h^{2h}$, $\boldsymbol{I}_{2h}^h$ and $\mathcal{A}_{2h}$ into (4.64) we immediately obtain the Fourier representation of $\boldsymbol{M}_h^{CGC}$.

Since

$$\rho_{loc}((\boldsymbol{S}_h(\theta))^{\nu_2}\boldsymbol{M}_h^{CGC}(\theta)(\boldsymbol{S}_h(\theta))^{\nu_1}) = \rho_{loc}(\boldsymbol{M}_h^{CGC}(\theta)(\boldsymbol{S}_h(\theta))^{\nu}) \ \ (\nu = \nu_1 + \nu_2) \tag{4.74}$$

we finally arrive at the two-grid convergence factor

$$\rho_{loc}(\nu;\tau) = \rho_{loc}(\boldsymbol{M}_h^{TGM}) = \sup\{\rho_{loc}(\boldsymbol{M}_h^{TGM}(\theta)) : \theta \in \Theta^{low}\} \tag{4.75}$$

with Θ^{low} as in (3.46). Here, ρ depends on ν and τ!

Using MAPLE we can compute the coefficients of the corresponding blocks $\boldsymbol{M}_h^{TGM}$ and the eigenvalues. In the following, we give the two-grid convergence factor in the limit case $h \to 0$ and optimal choices of parameter τ for special cases $\nu = 1$ and $\nu = 2$.

- For $\nu = 1$, we have

$$\begin{aligned} \rho_{loc}(1;\tau) &= \sup\{|-\frac{1}{2}\tau\cos^2(\theta) - \frac{1}{2}\tau + 1| : \theta \in [-\frac{\pi}{2}, \frac{\pi}{2})\} \\ &= \max\{|1-\tau|, |1-\frac{\tau}{2}|\} \end{aligned}$$

  The choice $\tau = 4/3$ is optimal in the following sense:

$$\inf\{\rho_{loc}(1;\tau) : 0 \le \tau \le 2\} = \rho_{loc}(1;\frac{4}{3}) = \frac{1}{3}.$$

- For $\nu = 2$, we have

$$\begin{aligned} \rho_{loc}(2;\tau) &= \sup\{|(\frac{3}{4}\tau^2 - \tau)\cos^2(\theta) + \frac{1}{4}\tau^2 - \tau + 1| : \theta \in [-\frac{\pi}{2}, \frac{\pi}{2})\} \\ &= \max\{(1-\tau)^2, (1-\frac{\tau}{2})^2\} \end{aligned}$$

  The choice $\tau = 4/3$ is optimal in the following sense:

$$\inf\{\rho_{loc}(2;\tau) : 0 \le \tau \le 2\} = \rho_{loc}(2;\frac{4}{3}) = \frac{1}{9}.$$

The optimal choices of τ in these two cases are the same with the choice in the smoothing analysis in (4.62). This is a strong indication that $\tau = 4/3$ is a good choice in the multigrid method. However, we are not able to predict the optimal choice of τ for the multigrid method.

4.5 Numerical Results

Next we present some numerical results for the domain $\Omega = (0, 1)$ and homogeneous desired state $y_d = 0$. The coarsest grid consists of only one inner point, i.e., with grid size $h_0 = 1/2$. For the first series of experiments the regularization parameter γ was set equal to 1. The starting values for $y_k^{(0)}$ and $p_k^{(0)}$ for the exact solution $y_k = 0$ and $p_k = 0$ were randomly chosen. The discretized problem was solved by a multigrid iteration with a V-cycle and m pre- and m post-smoothing steps. The multigrid iteration was performed until the Euclidean norm of the residual was reduced by a factor $\epsilon = 10^{-8}$.

Table 4.1 contains the number of unknowns n_k (total number of unknowns is $n_k + n_k$), the number of iterations it and the convergence rates q depending on the level k and the number m of smoothing steps.

		smoothing steps											
k	n_k	0+1		1+0		1+1		2+2		3+3		5+5	
5	63	26	0.49	27	0.49	14	0.26	9	0.11	7	0.074	6	0.045
6	127	26	0.49	27	0.49	14	0.26	9	0.11	7	0.074	6	0.045
7	255	26	0.50	27	0.50	14	0.26	9	0.11	7	0.074	6	0.045
8	511	26	0.50	27	0.50	14	0.26	9	0.11	7	0.074	6	0.045
9	1023	26	0.50	27	0.50	14	0.26	9	0.11	7	0.074	6	0.045

Table 4.1: V-cycle convergence rates with $\tau = 1$

In Section 4.1.3 we discussed the choice of the relaxation parameter τ. Table 4.2 shows the convergence rates for the overrelaxed smoother with $\tau = 1.33$. However, the convergence rates are much better than the rates for the original smoothing iteration with $\tau = 1$. The optimal choice of τ for smoothing operator and two-grid iteration is a good choice for multigrid method.

		smoothing steps											
k	n_k	0+1		1+0		1+1		2+2		3+3		5+5	
5	63	16	0.32	17	0.32	11	0.18	7	0.083	6	0.054	5	0.033
6	127	16	0.32	17	0.31	11	0.18	7	0.083	6	0.054	5	0.033
7	255	17	0.33	17	0.32	11	0.18	7	0.083	6	0.054	5	0.033
8	511	17	0.33	17	0.32	11	0.18	7	0.083	6	0.054	5	0.033
9	1023	17	0.33	17	0.33	11	0.18	7	0.083	6	0.054	5	0.033

Table 4.2: V-cycle convergence rates with $\tau = 1.33$

All numerical experientments shown so far were performed for the regularization parameter $\gamma = 1$. Table 4.3 shows the results of numerical experiments obtained at grid level 7 for values of γ ranging from 10 down to 10^{-5}. We can see that the behavior

of convergence rate q with respect to γ is as we have expected and the method proposed is robust in the regularization parameter γ.

	smoothing steps			
γ	1+1		10+10	
10	14	0.26	5	0.022
1	14	0.26	5	0.022
10^{-1}	14	0.26	5	0.022
10^{-2}	14	0.26	5	0.024
10^{-3}	14	0.28	5	0.029
10^{-4}	15	0.28	6	0.028
10^{-5}	15	0.28	5	0.027

Table 4.3: γ-dependence, $\tau = 1$

Finally, Table 4.4 and Table 4.5 show the convergence rates for W-cycle iteration using $\tau = 1$ and $\tau = 1.33$, respectively.

		smoothing steps											
k	n_k	0+1		1+0		1+1		2+2		3+3		5+5	
5	63	26	0.495	26	0.495	13	0.245	8	0.08	6	0.054	6	0.033
6	127	26	0.495	26	0.495	13	0.245	8	0.08	6	0.054	6	0.033
7	255	26	0.495	26	0.495	13	0.245	8	0.08	6	0.054	6	0.033
8	511	26	0.495	26	0.495	13	0.245	8	0.08	6	0.054	6	0.033
9	1023	26	0.495	26	0.495	13	0.245	8	0.08	6	0.054	6	0.033

Table 4.4: W-cycle convergence rates with $\tau = 1$

		smoothing steps											
k	n_k	0+1		1+0		1+1		2+2		3+3		5+5	
5	63	16	0.328	16	0.328	9	0.113	7	0.059	6	0.041	5	0.025
6	127	16	0.328	16	0.328	9	0.113	7	0.059	6	0.041	5	0.025
7	255	16	0.328	16	0.328	9	0.113	7	0.059	6	0.041	5	0.025
8	511	16	0.328	16	0.328	9	0.113	7	0.059	6	0.041	5	0.025
9	1023	16	0.328	16	0.328	9	0.113	7	0.059	6	0.041	5	0.025

Table 4.5: W-cycle convergence rates with $\tau = 1.33$

Chapter 5

Conclusion

In this thesis we first study the smoothing factor and two-grid convergence factor of 1D poisson problem using damped Jacobi iteration as smoother. Fourier two-grid analysis for this model problem was described in [18], but for fixed relaxation parameter $\omega = 1/2$. Here we generalize the Fourier two-grid analysis for all $\omega \in [0, 1]$ and study the optimal choices of ω when the total smoothing steps are equal to 1 or 2. In comparison, local Fourier smoothing and two-grid analysis is also presented for model problem. And we get the same results for both smoothing factor and two-grid convergence factor in the asymptotic sense. Also, from the theoretical point of view the connections and differences of Fourier analysis and LFA are illustrated.

The main part of this work is application to an optimal control problem where a regularization parameter γ is involved. It would be desirable to achieve robustness of the smoother proposed by W.Zulehner with respect to this regularization parameter. Finite element discretization results in two-by-two block system which makes the convergence analysis more complicated than the scalar 1D model problem. We obtain the asymptotic smoothing factor and observe its independence with respect to the regularization parameter γ. However, we cannot conclude from the robustness of the smoothing factor that the two or the multigrid methods are robust. Local Fourier two-grid analysis is derived and two-grid convergence factor for special cases are obtained. Since the Fourier two-grid analysis is very technical, we describe the road map to derive the two-grid convergence rates by Fourier analysis. Numerical results here show the robustness.

The optimal control problem analyzed in Chapter 4 is quite similar to the mixed formulation of the biharmonic equation. Indeed, for the first biharmonic boundary value problem in 1D (beam equation)

$$-u^{(4)} = f \quad \text{in} \quad \Omega, \quad u = u' = 0 \quad \text{at} \quad \Gamma, \tag{5.1}$$

we obtain the following mixed variational problem by introducing the new unknown

function $w = u''$: Find $(w, u) \in V \times W = H^1(\Omega) \times H_0^1(\Omega)$ such that

$$\begin{aligned} a(w,v) + b(u,v) &= 0 \qquad \text{for all} \quad v \in V, \\ b(w,q) &= \langle G, q \rangle \quad \text{for all} \quad q \in W, \end{aligned} \tag{5.2}$$

with

$$\begin{aligned} a(w,v) &= \int_0^1 w(x)v(x)dx, \\ b(u,v) &= \int_0^1 u'(x)v'(x)dx, \\ \langle G, q \rangle &= -\int_0^1 f(x)q(x)dx. \end{aligned}$$

We again subdivide the interval $\Omega = (0,1)$ into n parts with grid size $h = \frac{1}{n}$ and discrete by continuous and piecewise linear finite elements:

$$\begin{aligned} V_h &= \{v \in C(\bar{\Omega}) : v|_T \in P_1 \text{ for all } T \in \mathcal{T}_h\}, \\ W_h &= \{q \in C(\bar{\Omega}) : q|_T \in P_1 \text{ for all } T \in \mathcal{T}_h, q(0) = q(1) = 0\}. \end{aligned}$$

So we obtain the following discrete variational problem: Find $w_h \in V_h$ and $u_h \in W_h$ such that

$$\begin{aligned} a(w_h,v) + b(u_h,v) &= 0 \qquad \text{for all} \quad v \in V_h, \\ b(w_h,q) &= \langle G, q \rangle \quad \text{for all} \quad q \in W_h. \end{aligned}$$

By introducing the same standard nodal basis for all unknowns, we finally obtain the following saddle point problem in matrix-vector notation:

$$\mathcal{A}_h \begin{pmatrix} \underline{w}_h \\ \underline{u}_h \end{pmatrix} = \begin{pmatrix} 0 \\ \underline{g}_h \end{pmatrix} \quad \text{with} \quad \mathcal{A}_h = \begin{pmatrix} M_h & K_h^T \\ K_h & 0 \end{pmatrix} \tag{5.3}$$

where M_h is the $(n+1) \times (n+1)$ mass matrix

$$M_h = \frac{h}{6} \begin{bmatrix} 2 & 1 & & & & & \\ 1 & 4 & 1 & & & & \\ & 1 & 4 & 1 & & & \\ & & 1 & \ddots & \ddots & & \\ & & & \ddots & \ddots & 1 & \\ & & & & 1 & 4 & 1 \\ & & & & & 1 & 2 \end{bmatrix}_{(n+1)\times(n+1)} \tag{5.4}$$

and K_h is the $(n-1)\times(n+1)$ stiffness matrix

$$K_h = \frac{1}{h}\begin{bmatrix} -1 & 2 & -1 & & & & & \\ & -1 & 2 & -1 & & & & \\ & & -1 & \ddots & \ddots & & & \\ & & & \ddots & \ddots & -1 & & \\ & & & & -1 & 2 & -1 & \\ & & & & & -1 & 2 & -1 \end{bmatrix}_{(n-1)\times(n+1)} . \tag{5.5}$$

The main difference of optimal control problem and the biharmonic problem is: the stiffness matrix K_h in optimal control problem is a square matrix whereas in biharmonic problem is a rectangular matrix. This is due to the difference in the boundary conditions. Apply LFA to biharmonic problem will give the same results as for optimal control problem since we neglect the boundary conditions in LFA. This is not the result we want to obtain. Future work will focus on the Fourier analysis of this problem.

Bibliography

[1] G. Astrakhantsev. An iterative method for solving elliptic net problems. *USSR Comput. Math. and Math. Physics*, 11(2):171–182, 1971.

[2] N. Bakhvalov. On the convergence of a relaxation method with natural constraints on the elliptic operator. *Zh. Vychisl. Mat. Mat. Fiz*, 6:861–885, 1966.

[3] J. Bramble. *Multigrid methods*. Chapman & Hall/CRC, 1993.

[4] A. Brandt. Multi-level adaptive technique/MLAT/ for fast numerical solution to boundary value problems. In *International Conference on Numerical Methods in Fluid Mechanics, 3 rd, Paris, France*, pages 82–89, 1973.

[5] A. Brandt. Multi-level adaptive techniques. *IBM IJ Watson Research Center, Yorktown Heights, New York. IBM Research Report RC6026*, 1976.

[6] A. Brandt. Multi-level adaptive solutions to boundary-value problems. *Math. Comp.*, 31(138):333–390, 1977.

[7] A. Brandt. Multigrid solvers for non-elliptic and singular-perturbation steady-state problems. *The Weizmann Institute of Science, Rehovot, Israel*, 1981.

[8] A. Brandt. Guide to multigrid development. *Multigrid methods*, 960:220–312, 1982.

[9] A. Brandt. Rigorous quantitative analysis of multigrid, I: Constant coefficients two-level cycle with L2-norm. *SIAM Journal on Numerical Analysis*, pages 1695–1730, 1994.

[10] W. Briggs, V. Henson, and S. McCormick. A Multigrid tutorial 2nd ed. *SIAM, Philadelphia*, 2000.

[11] R. Fedorenko. A relaxation method for solving elliptic difference equations. *USSR Comput. Math. and Math. Phys*, 1(5):1092–1096, 1961.

[12] R. Fedorenko. The speed of convergence of one iterative process. *USSR Comp. Math. and Math. Physics*, 4:227–235, 1964.

[13] W. Hackbusch. Ein iteratives Verfahren zur schnellen Auflosung elliptischer Randwertprobleme. *Report 76-12, Institute for Applied Mathematics, University of Cologne, West Germany*, 1976.

[14] W. Hackbusch. On the convergence of a multi-grid iterations applied to finite element equations. *Report 77-8, Institute for Applied Mathematics, University of Cologne, West Germany*, 1977.

[15] W. Hackbusch. Convergence of multi-grid iterations applied to difference equations. *Mathematics of Computation*, pages 425–440, 1980.

[16] W. Hackbusch. On the convergence of multi-grid iterations. *Beitrage zur Numer. Math*, 9:213–239, 1981.

[17] W. Hackbusch. Multi-grid convergence theory. In *Multigrid Methods: Proceedings of the Conference Held at Köln-Porz, November 23-27, 1981*, page 177. Springer-Verlag, 1982.

[18] W. Hackbusch. *Multi-grid methods and applications*. Springer, 1985.

[19] W. Hackbusch and U. Trottenberg. Multigrid Methods, Lecture Notes in Math., Vol. 960, 1982.

[20] V. Korneev. Finite Element Schemes of High Order of Accuracy, Leningrad University, Leningrad, 1977.

[21] K. Stüben and U. Trottenberg. Multigrid methods: fundamental algorithms, model problem analysis and applications. In *Multigrid methods (Cologne, 1981)*, volume 960 of *Lecture Notes in Math.*, pages 1–176. Springer, Berlin, 1982.

[22] K. Stueben and U. Trottenberg. On the construction of fast solvers for elliptic equations. *In Von Karman Inst. for Fluid Dyn. Computational Fluid Dyn. 161 p (SEE*, 83, 1982.

[23] C.-A. Thole and U. Trottenberg. A short note on standard parallel multigrid algorithms for 3d problems. *Appl. Math. Comput.*, 27(2):101–115, 1988.

[24] F. Tröltzsch. *Optimale Steuerung partieller Differentialgleichungen: Theorie, Verfahren und Anwendungen*. Vieweg Verlag, 2005.

[25] U. Trottenberg, C. W. Oosterlee, and A. Schüller. *Multigrid*. Academic Press Inc., San Diego, CA, 2001. With contributions by A. Brandt, P. Oswald and K. Stüben.

[26] P. Wesseling. *An introduction to multigrid methods*. Wiley Chichester, 1992.

[27] R. Wienands and W. Joppich. *Practical Fourier analysis for multigrid methods*, volume 4 of *Numerical Insights*. Chapman & Hall/CRC, Boca Raton, FL, 2005. With 1 CD-ROM (Windows and UNIX).

[28] D. Young Jr. Iterative methods for solving partial differential equations of elliptic type (Ph. D. thesis), Harvard University, Cambridge, Mass, 1950.

Curriculum Vitae

Name: Zhou Yao

Nationality: China

Date of Birth: January 7th, 1986

Place of Birth: Hubei Province, China

Education:

2003 - 2007	Bachelor Study, Informatics and Computational Mathematics Beihang University
2007 - 2008	Graduate Study, Applied Mathematics Beihang University Master
2008 - 2009	International Master's Program for Informatics Austria, Hagenberg, Johannes Kepler University (JKU)

Special Activities:

November 2006	China Undergraduate Mathematical Contest in Modeling Second Prize in China
March 2007	America Mathematical Contest in Modeling Honorable Mention.

Eidesstattliche Erklärung

Ich erkläre an Eides statt, dass ich die vorliegende Masterarbeit selbständig und ohne fremde Hilfe verfasst, andere als die angegebenen Quellen und Hilfsmittel nicht benutzt bzw. die wörtlich oder sinngemäß entnommenen Stellen als solche kenntlich gemacht habe.

Linz, July 2009

_____

Yao Zhou